# SuperNEMO Conceptual Design Report

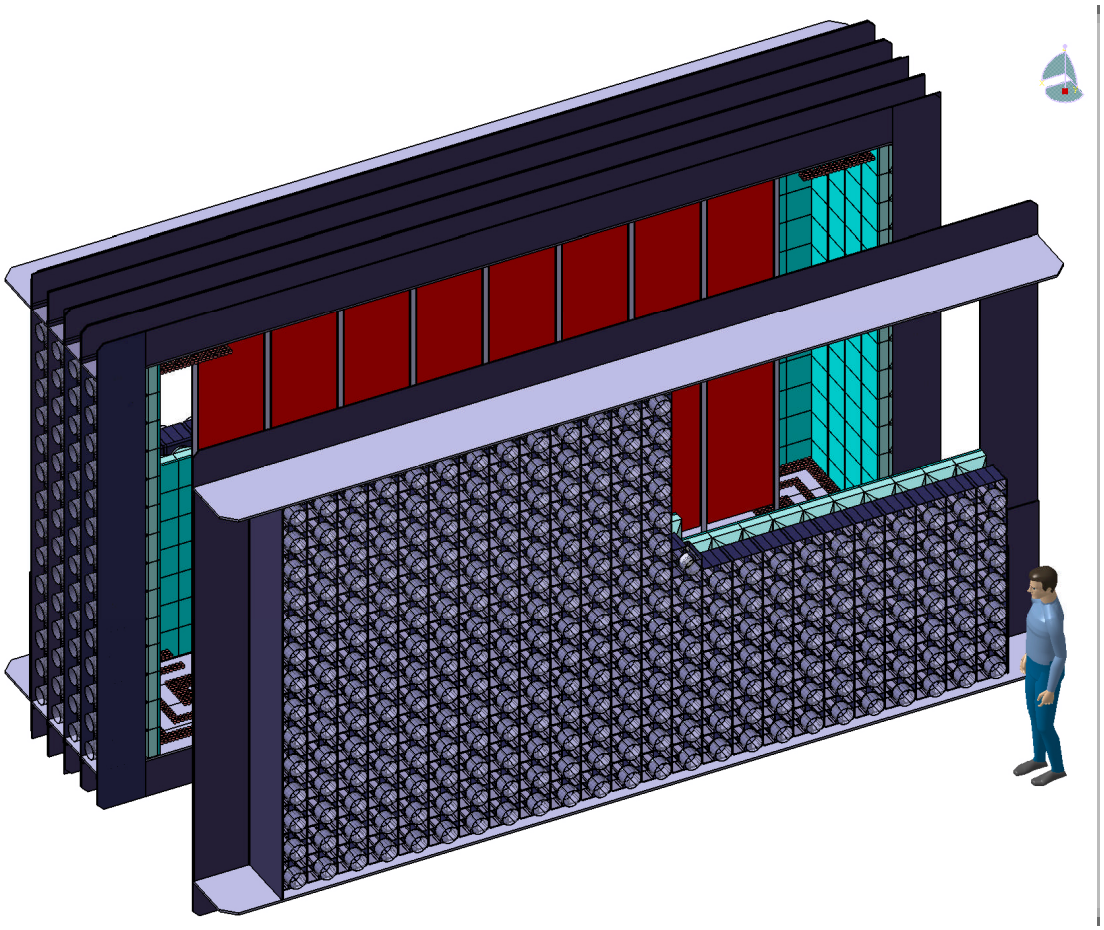

*The SuperNEMO Collaboration*

# Table of Contents

**Comments on this Document**

**The purpose of this document is to describe the conceptual design of the SuperNEMO experiment. It is a working document that will evolve as the project progresses. Eventually it will transform into a detailed technical design report (TDR). At the time of writing (April 2010), some elements of the design are more advanced than the others. In particular, the tracker module design, which is a sole responsibility of the UK group, is closer to the completion. Consequently, this document, at the moment, focuses on the tracker and other related elements of the design in much more detail.**
**The document addresses the design of the first super-module (the Demonstrator) reflecting the current phase of the experiment. The final design of the SuperNEMO detector will be produced based on the results obtained with the Demonstrator module.**

# Executive Summary

The SuperNEMO experiment will search for neutrinoless double beta decay (DBD). Its observation will be direct evidence that neutrinos are of Majorana type i.e. that neutrinos and anti-neutrinos are identical. The observation of neutrinoless DBD would furthermore yield information on the absolute neutrino mass scale and hierarchy, which are not directly obtainable from oscillation experiments. The SuperNEMO collaboration consists of ~90 scientists from the UK, France, Spain, Russia, the Czech Republic, US and Japan.

SuperNEMO follows and improves the tried and tested technology developed by a series of NEMO experiments. The basic components will include ~100 kg of source foils, scintillator calorimetry and a Geiger wire chamber to enable both energy measurement and tracking, producing an unambiguous topological signature of the decay electrons from the source. The detector's ability to measure any DBD isotope and the topological signature are distinct features of SuperNEMO that are not present in any other future DBD experiment. The baseline isotope choice for SuperNEMO is $^{82}$Se. The experiment will reach a sensitivity to the Majorana neutrino mass of 50-100 meV in 5 years of running with 100 kg isotope (500 kg yr exposure). SuperNEMO is one of three projects (together with CUORE and GERDA) on the European road map for future generation neutrinoless DBD experiments (ASPERA).

The SuperNEMO collaboration has just finished a four-year R&D/design study. The study has successfully addressed three main challenges: improvement of the calorimeter energy resolution, radiopurity of the source foils and optimization of the tracker detector for large-scale production under low background requirements.
SuperNEMO will require large scale production of detector components under challenging ultra-low background requirements. Between full-scale detector construction and the current R&D, there has to be an intermediate step to demonstrate the feasibility of mass production for such a detector.
SuperNEMO is now entering its construction phase and the first super-module (the Demonstrator module) will be ready to be installed in the LSM underground laboratory in 2013. Apart from the technology demonstration, the first super-module will be able to produce a competitive physics result covering the sensitivity of the recent claim made by Klapdor-Kleingrothaus [1].

This document lays out the details of the Demonstrator module conceptual design. It includes the information on major milestones and the schedule.

# 1.0 Physics case for SuperNEMO

## 1.1 Double beta decay and BSM physics

Neutrinoless double beta decay (0νββ) is a lepton-number-violating transition in which the parent nucleus (Z,A) decays to the daughter nucleus (Z+2,A) emitting two electrons. A related transition allowed in the standard model called two-neutrino double beta decay (2νββ) is accompanied by the emission of two electrons and two anti-neutrinos.

The development of effective field theory and grand unification schemes has led to the expectation that, unlike all the other fermions of the standard model, neutrinos are identical to their anti-particles and have non-zero rest mass [2]. The latter was spectacularly demonstrated by neutrino oscillation experiments [3]. However neutrino oscillations can only measure the difference between squared neutrino masses and not their absolute value. Thus, the search for 0νββ addresses two of the most fundamental questions of particle physics:

1. The nature of the neutrino (Majorana or Dirac).
2. The absolute value of the neutrino mass.

0νββ decay is the only practical way to answer the first question and is probably the most sensitive method to measure the absolute neutrino mass in a laboratory environment.

There are different mechanisms that can lead to 0νββ. The mechanism most commonly discussed is the one shown in Figure 1.1, in which a light Majorana neutrino is exchanged. In this case, the probability (or the inverse half-life) of the process can be expressed as:

$$\left(T_{1/2}^{0\nu}\right)^{-1} = G^{0\nu}\left|M^{0\nu}\right|^2\left\langle m_\nu\right\rangle^2 \qquad (1)$$

where $G^{0\nu}$ is the phase space and $M^{0\nu}$ is the nuclear matrix element for the transition. $\left\langle m_\nu\right\rangle$ is the effective Majorana neutrino mass, described below.

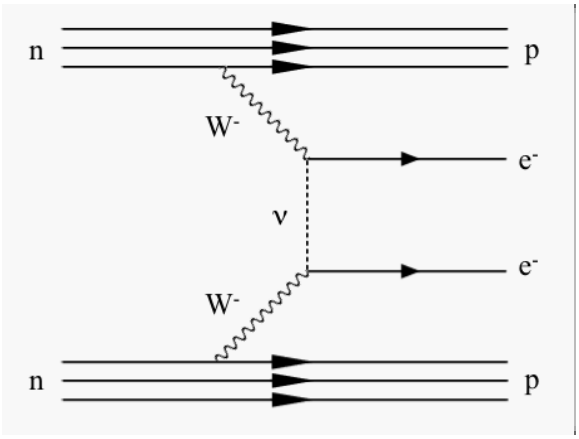


*Figure 1.1: Double beta decay via the exchange of a Majorana type neutrino.*

However other mechanisms are possible, to name a few:

1. A right handed (V+A) weak current interaction mediated by a $W_R$ boson.
2. Emission of a massless Goldstone boson, the Majoron.
3. R-parity violating SUSY models.
4. Exchange of a doubly-charged Higgs boson.

Therefore the $\langle m_\nu \rangle$ term in Equation 1 should be treated as a lepton number violating parameter, which can have a different form according to the underlying physics mechanism. Clearly the focus now is on finding the first clear evidence for this process but, once this is established, the most important question will be to disentangle the physics behind 0νββ.

Assuming the neutrino mass is the dominant mechanism, the information from 0νββ, neutrino oscillations and kinematic neutrino mass measurements can be combined to create a complete picture of neutrino properties. The effective mass is given by:

$$\langle m_\nu \rangle = m_1|U_{e1}|^2 + m_2|U_{e2}|^2 e^{i\langle_{21}} + m_3|U_{e3}|^2 e^{i\langle_{31}} \qquad (2)$$

where $m_i$ are the mass eigenstates, $U_{ei}$ are elements of the PMNS neutrino mixing matrix derived from oscillation experiments, $\langle_i$ are the two Majorana CP-violating phases. As one can see from Fig. 1.2, a measurement of $\langle m_\nu \rangle$ and the lightest neutrino mass (which, for example, can be obtained from tritium end-point experiments combined with neutrino oscillation results) will provide an answer to the question of the neutrino mass hierarchy. Light may also be shed on the question of CP-violation in the neutrino sector.

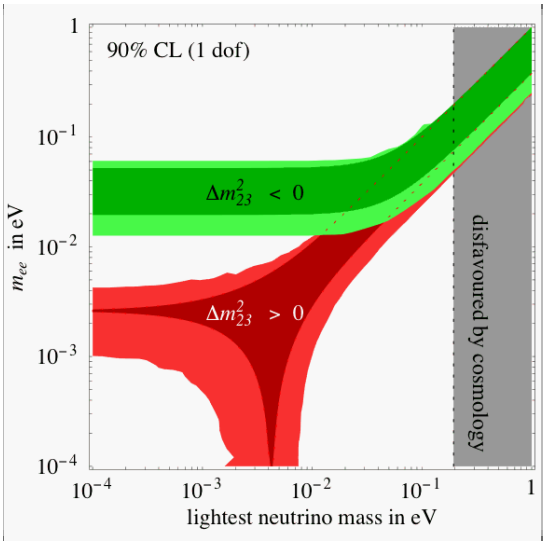


*Figure 1.2 : A plot of the effective double-beta decay neutrino mass as a function of the lightest neutrino mass for normal (red) and inverse (green) hierarchies. From [4]*

The accuracy of the $\langle m_\nu \rangle$ determination depends on the phase space factor $G^{0\nu}$ and the nuclear matrix element $M^{0\nu}$. While the phase space factor is known precisely, there are significant uncertainties associated with $M^{0\nu}$. The calculation of nuclear matrix elements is extremely difficult and requires input from nuclear theory. The two main techniques for calculating the matrix elements are the Quasi-particle Random Phase Approximation (QRPA) and the Nuclear Shell Model (NSM). There has been significant progress in both approaches in recent years and the uncertainties are shrinking. Nevertheless, we have no way of knowing which calculation gives the right result, at least until the process is discovered experimentally. The existence of NME uncertainties also significantly strengthens the case for searching for 0νββ in *several different nuclei*.

We note that the above-mentioned uncertainties do not make 0νββ less appealing, since its discovery will probe directly physics beyond the standard model (through full lepton number

violation). Also, as was shown in [5], the discovery of 0νββ implies unambiguously that neutrinos are Majorana particles, regardless of the dominating mechanism.

Alongside 0νββ, it is important to study 2-neutrino double beta decay. The half-life for this process is given by:

$$\left(T_{1/2}^{2\nu}\right)^{-1} = G^{2\nu}\left|M^{2\nu}\right|^2 \qquad (3)$$

By measuring $T_{1/2}^{2\nu}$, one can therefore determine the corresponding matrix element $M^{2\nu}$ experimentally. Although there is no one-to-one correspondence between $M^{0\nu}$ and $M^{2\nu}$, the information obtained from 2νββ leads to a development of theoretical schemes that can be used for both 0νββ and 2νββ calculations. In addition, 2νββ is the ultimate background for 0νββ and an accurate knowledge of the 2νββ spectrum shape and other characteristics is of paramount importance to understand this background. The measurement and characterization of the 2νββ process is another unique feature of the NEMO approach.

There are over 30 isotopes that can undergo ββ decay but only 9 of them are "serious contenders". An important criterion for the isotope selection is the $Q_{\beta\beta}$ value of the process, with higher values being preferred. One reason for this is a strong dependence of the phase space and therefore the probability of the process on $Q_{\beta\beta}$ ($G^{0\nu} \propto Q_{\beta\beta}^5, G^{2\nu} \propto Q_{\beta\beta}^{11}$). The other reason is due to the natural background, which is mostly situated below a 2.6 MeV line of $^{208}$Tl (a progeny of the $^{232}$Th decay-chain). Other considerations include the isotope's natural abundance, feasibility of enrichment and purification, the half-life of the 2νββ decay mode, etc. The main isotopes considered in current and future ββ experiments and their main characteristics are shown in **Error! Reference source not found.**

| **Isotope** | **%** | $Q_{\beta\beta}$ **(keV)** | $T_{1/2}^{2\nu}$ **(10 $^{19}$yrs)** |
|---|---|---|---|
| $^{48}$Ca | 0.19 | 4271 | 4.2 ± 0.5* |
| $^{76}$Ge | 7.4 | 2039 | 150 ± 10 |
| $^{82}$Se | 9.2 | 2995 | 9.6 ± 1.0* |
| $^{96}$Zr | 2.8 | 3350 | 2.35 ± 0.24* |
| $^{100}$Mo | 9.6 | 3034 | 0.71 ± 0.05* |
| $^{116}$Cd | 7.49 | 2802 | 2.8 ± 0.3* |
| $^{130}$Te | 33.8 | 2533 | 69 ± 13* |
| $^{150}$Nd | 5.6 | 3367 | 0.9 ± 0.06* |
| $^{136}$Xe | 8.9 | 2479 | > 1000 |

*Table 1.1 : Isotopes used in the search for neutrinoless double-beta decay. The second column shows the natural abundance of the isotope, the third column the energy released in the double-beta transition and the final column shows the half-life of the 2-neutrino decay mode.*

* - Results from the NEMO-III experiments [6].

## 1.2 Experimental approaches

The spectra of the energy sum of two electrons emitted in the decay are shown in Figure 1.3 for different mechanisms of ββ decay. The standard model 2νββ decay has a continuous spectrum due

to anti-neutrinos carrying away a part of the energy, while the 0νββ decay has a distinct delta-function peak (smeared by the energy resolution of the detector) for all decay modes except for the one accompanied by Majoron emission.

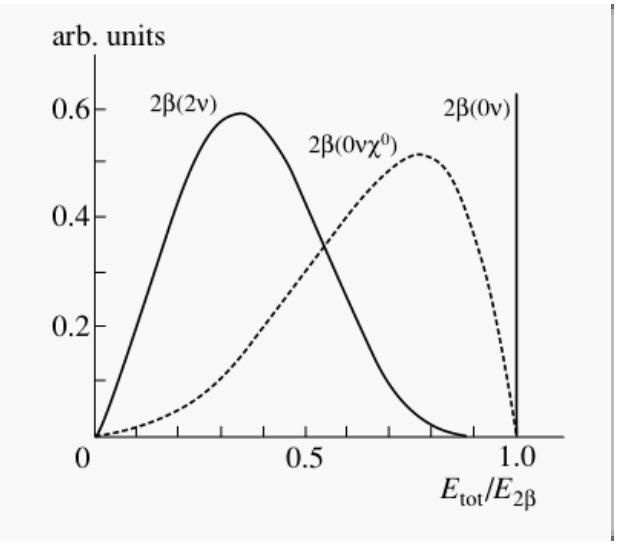


*Figure 1.3 : The spectra of the summed electron energies, as a fraction of the total energy available in the decay. The standard model 2ν decay mode produces a continuous spectrum, while the 0ν mode is a delta-funtion at 1. Majoron emission can generate different spectra. From [7].*

Searching for 0νββ decay is difficult. Most ββ experiments face U and Th decay-chain isotopes as their limiting background component. The problem comes from the extreme rarity of the process. The experiments carried out so far have established that the half-life of 0νββ is greater than ~$10^{25}$ years, while U and Th half lives are of the order of $10^{10}$ years. A continuous spectrum arising from Compton scattered gamma rays, beta rays and alpha particles from the naturally occurring decay chains can overwhelm any peak for the 0νββ signal. The most dangerous isotopes are $^{214}$Bi ($Q_\beta$=3.27 MeV) and $^{208}$Tl ($Q_\beta$=4.99 MeV) from $^{238}$U and $^{232}$Th decay chains respectively. The contamination is present in the detector materials and in the laboratory outside the detector. In addition, cosmic ray muons, either directly or through neutron production, can create a background mimicking the 0νββ signal. The ββ detectors are therefore always placed underground and extreme care is taken during the materials selection process.

There are two distinct experimental approaches in the search for 0νββ. The first approach is when the ββ source is itself the detector, such as in Germanium detectors or $TeO_2$ bolometers. The other is when the source is not part of the detector and a multi-purpose detector suite is arranged around it. The first type is characterised by high efficiency and an impressive energy resolution. This excellent energy resolution allows a powerful discrimination between 2νββ and 0νββ events but may not be sufficient to eliminate non-ββ backgrounds since *any* energy deposition in the end-point region will fake the signal. In addition, this approach does not produce a "smoking gun" signature of the ββ signal and restricts the choice to a single isotope. The second approach has a worse energy resolution but the advantage of particle identification and event topology recognition. The topology and individual electron energy reconstruction may also be used to disentangle the underlying physics mechanism of 0νββ. It is this approach which is adopted by the NEMO-III and SuperNEMO experiments.

## 1.3 NEMO-III

The SuperNEMO design follows and improves upon the tried and tested technology of the previous NEMO experiments, in particular the technology employed in the NEMO-III detector currently

taking data in the Modane underground laboratory (LSM) at a depth of 4800 m.w.e. (metres of water equivalent).

The detector is cylindrically subdivided into 20 identical sectors containing thin source foils (~ 50 mg/cm$^2$) situated in the middle of the tracking volume surrounded by the calorimeter. The source foils are composed 6.9 kg of $^{100}$Mo, 1 kg of $^{82}$Se and smaller amounts of $^{116}$Cd, $^{150}$Nd, $^{96}$Zr, $^{48}$Ca and $^{130}$Te. One of the sectors contains a "blank" copper foil for external background evaluation. Observation of the ββ decay is accomplished by fully reconstructing the tracks of the two electrons and measuring their energy. A tracking chamber, containing 6180 open drift cells, operates in the Geiger mode and provides a vertex resolution of about 1 cm. A 25 Gauss magnetic field is used to curve the tracks for charge identification. A calorimeter consisting of 1940 plastic scintillator blocks coupled to Hamamatsu low radioactive PMTs gives an energy resolution of 14% to 17% (FWHM) at 1 MeV. A time resolution of 250 ps allows excellent suppression of the external background due to electrons crossing the detector. The detector is capable of identifying e-, e+, gamma and alpha particles and allows good discrimination between signal and background events. The detector is covered by two layers of passive shielding against external gamma rays and neutrons.

NEMO-III is in its physics exploitation phase and has produced a series of world class ββ measurements [6]. Apart from delivering important physics results, NEMO-III is an invaluable test bench for SuperNEMO. NEMO-III has proved to be crucial to our understanding of the backgrounds that we may expect to see in SuperNEMO. It is anticipated that the NEMO-III detector will continue to take data until the end of 2010 and will reach a sensitivity to the Majorana effective mass at the level of 300-600 meV.

## 1.4 SuperNEMO detector

SuperNEMO will build upon the NEMO-III technology choice of combining calorimetry and tracking but will have a planar geometry. The baseline SuperNEMO design envisages about twenty identical modules, each housing around ~5 kg of isotope. A preliminary design of a SuperNEMO detector module is shown in Figure 1.4. The source is a thin (~ 40 mg/cm$^2$) foil inside the detector. It is surrounded by a gas tracking chamber followed by calorimeter walls. The tracking volume contains around 2000 wire drift cells operated in Geiger mode which are arranged in nine layers parallel to the foil. The calorimeter is divided into 550 plastic scintillator hexagonal blocks (~ 27 cm diameter) which cover most of the detector outer area and are coupled to low radioactive 8" PMTs.

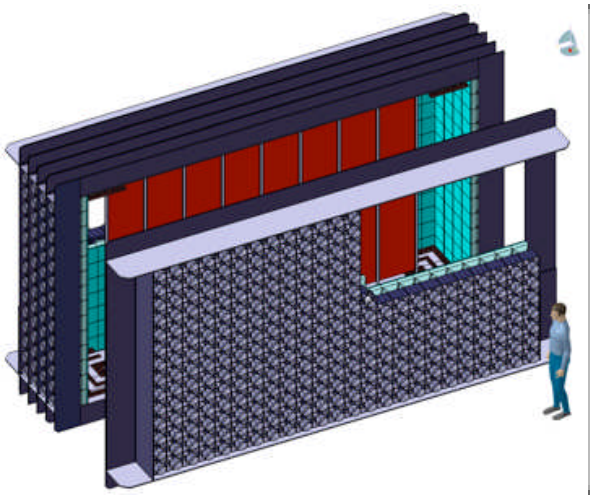

*Figure 1.4 : schematic of a proposed SuperNEMO module showing the source foil (red) surrounded by a tracking volume and scintillator blocks read out by PMT's.*

The choice of isotope for SuperNEMO is aimed at maximising the neutrinoless signal over the background of two-neutrino double beta decay and other nuclear decays mimicking the process. Therefore the isotope must have a long two-neutrino half-life, a high endpoint energy and a large phase space factor. The possibility of isotopic enrichment on a large scale is also a factor in selecting the isotope. The baseline candidate isotope for SuperNEMO is $^{82}$Se. The SuperNEMO collaboration is also investigating the possibility of enriching large amounts of $^{150}$Nd via the method of atomic vapour laser isotope separation.

## 1.5 SuperNEMO sensitivity

SuperNEMO is one of three projects (together with CUORE and GERDA) on the European road map for future generation neutrinoless DBD experiments (ASPERA). These experiments, as well as other experiments such as EXO, SNO+, COBRA etc. aim to reach sensitivity to a Majorana neutrino mass at the level of 0.05 eV by 2017-2020. There is inevitably a healthy competition between these experiments, but they are actually very complementary as they measure different isotopes, which is crucial in light of existing uncertainties in nuclear matrix element (NME) calculations and due to the elusive nature of the signal.

The sensitivity of SuperNEMO has been studied extensively during the design study phase [8]. A full chain of GEANT4 based simulation software has been developed and commissioned and the sensitivity was studied as a function of various detector parameters such as the calorimeter energy resolution, source foil radiopurity, tracking detector configuration etc. Simulation results have provided a key input into the design details of the Demonstrator module.

The SuperNEMO approach is unique as it is the ***only*** next generation $0\nu\beta\beta$ experiment that uses the topological signature to select the $\beta\beta$ events. The ***unique*** features of SuperNEMO are:

1. Source and detector are separated. This allows a measurement of any $\beta\beta$ isotope or several isotopes at the same time.
2. Topological reconstruction of two electron tracks emitted from the same vertex.
3. Efficient particle identification (e-, e+, gamma rays, alpha-particles).
4. Measurement of most final state observables: individual electron energies and angular distributions between two electrons.

This approach gives a very powerful rejection of non-$\beta\beta$ background events, leaving the $2\nu\beta\beta$ decay as one of the main backgrounds for SuperNEMO. Moreover, it produces a "smoking gun"

signature of the ββ signal. If 0νββ is discovered with sufficient statistics, the measurement of the individual electron energies and angular distributions may enable us to disentangle the underlying physics mechanism [8].

A key concept of the SuperNEMO physics strategy is an attempt to produce as open minded a measurement of 0νββ as possible, without restricting the physics of the process to a particular mechanism. For example, if Majoron emission is indeed the dominating mechanism, then the spectrum of the sum of the two electron's energies is continuous and energy resolution becomes less important, while non-ββ background rejection is still crucial. Indeed, the currently running NEMO-III experiment holds the world's best limits on this mechanism of 0νββ decay.

An important feature of the SuperNEMO design is the possibility of a "last minute change" of the isotope if necessary. For example, if CUORE observes a significant signal at a relatively early stage (e.g. $\langle m_\nu \rangle \geq 0.1$ eV), then $^{130}$Te can be introduced in SuperNEMO and all characteristics of the decay (ββ "smoking gun" signature, individual electron energies, angular correlations) can be studied and, possibly, the underlying physics mechanism uncovered.

## 1.6 Physics reach studies

The SuperNEMO software system, SNSW, allows for the simulation, reconstruction and analysis of double beta decay and background events in the SuperNEMO detector, thus facilitating detector optimization and physics reach studies.

An overview of the main elements of the SuperNEMO software structure and data flow is shown in Fig 1.5. The elements shown are:

- SNGENBB is an event generator for the double beta decay modes of various isotopes. It can also generate all major background event types.
- SNVERTEX allows the event vertices to be located in any region of the detector (e.g. foil, gas, tracker wires, etc.).
- A Geant4 based detector simulation is implemented in the SNOVA package. Various geometries can be modelled including the baseline and alternative bar (single module and 'sandwich') calorimeter designs.
- SUNAMI provides digitization of the detector response for the tracker Geiger cells and for the calorimeter.
- The next two elements of the chain are reconstruction software: CATS implements a cellular automaton algorithm to search for track patterns, NEMORA uses the Kalman filter to fit the tracks and performs the final event reconstruction.
- The analysis package provides a set of functions to perform high level analyses such as track quality checks, topology analysis, time-of-flight analysis etc. There are analysis modes to select good ββ candidate events and functionality to select for multiple electrons and gammas for calibration studies.

In addition, there are also general I/O and track fitting libraries (BHEP and RECPACK) and visualisation software.

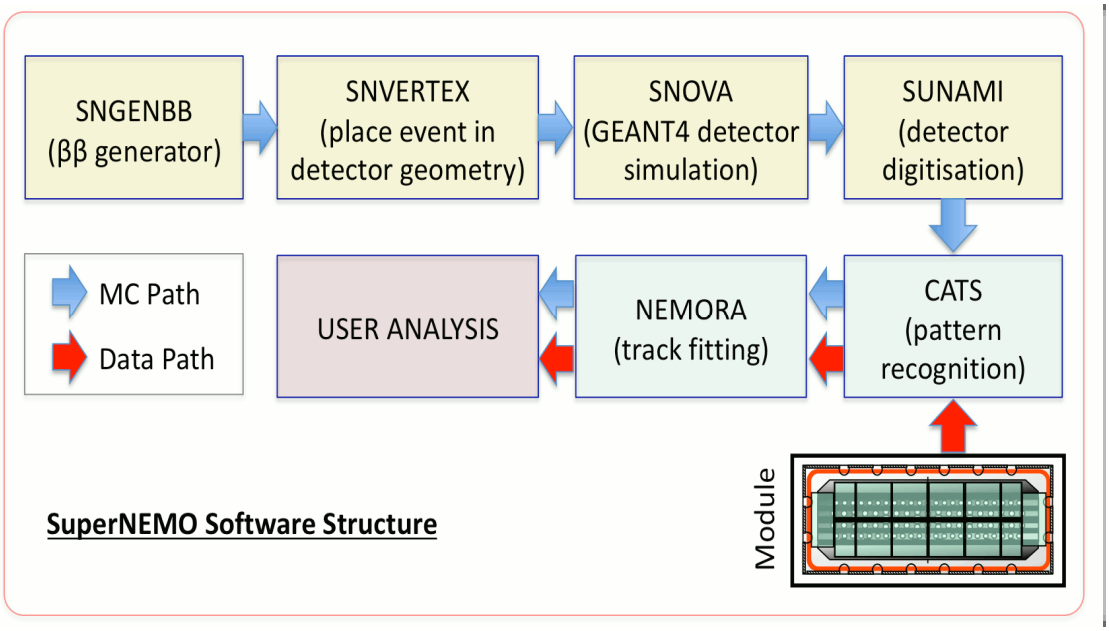


*Figure 1.5 : Schematic of the SuperNEMO software structure showing the major software packages and data flow.*

The software is maintained on a central (svn) repository. Documentation is similarly available (wiki). A software management package, PACKMAN, handles automatic processing of both single software packages and 'releases', thus allowing the user to extract the required software modules from the repository, configure, compile and install them in a straightforward and unified way. An infrastructure, SNgrid, enables GRID usage in a reasonably transparent manner. The Ganga GRID user interface is utilized and allows large scale GRID simulations, including multi-job creation, preparation and submission, job monitoring, data saving and merging, and also incorporates a data storage scheme. Ganga allows the user to configure, prepare and monitor applications submitted to a variety of resources. The SuperNEMO VO (Virtual Organization), which utilises the LHC File Catalogue (LFC), has the use of GRID computing facilities across Europe.

For the next phase of the project, software components for handling real data from the Demonstrator module will be implemented together with associated databases for geometry, calibration and data file catalogues etc.

Physics sensitivity studies have provided crucial inputs to the detector design (see elsewhere in this report). The parameters studied have included the tracker cell size and layout, the calorimeter block size, thickness, packing fraction and resolution, the source foil height and thickness, magnetic field and the efficiency of the gamma veto. The effect of backgrounds has also been studied and used to set target values for radioactive contaminations. The backgrounds modelled include the five main channels: $2\nu\beta\beta$, $Bi^{214}$ and $Tl^{208}$ in the foil, and $Bi^{214}$ and $Tl^{208}$ in the gas.

The sensitivity for the baseline geometry as a function of the calorimeter energy resolution (at 1MeV) and as a function of exposure (kg yrs), for various source foil thicknesses, is shown in Fig. 1.6. (The baseline design assumes 15cm deep blocks, gamma veto, 500 kg yrs, $^{82}Se$ source.) The target sensitivity of ~$10^{26}$ yrs (50-110 meV) has been demonstrated with realistic simulations of the detector effects.

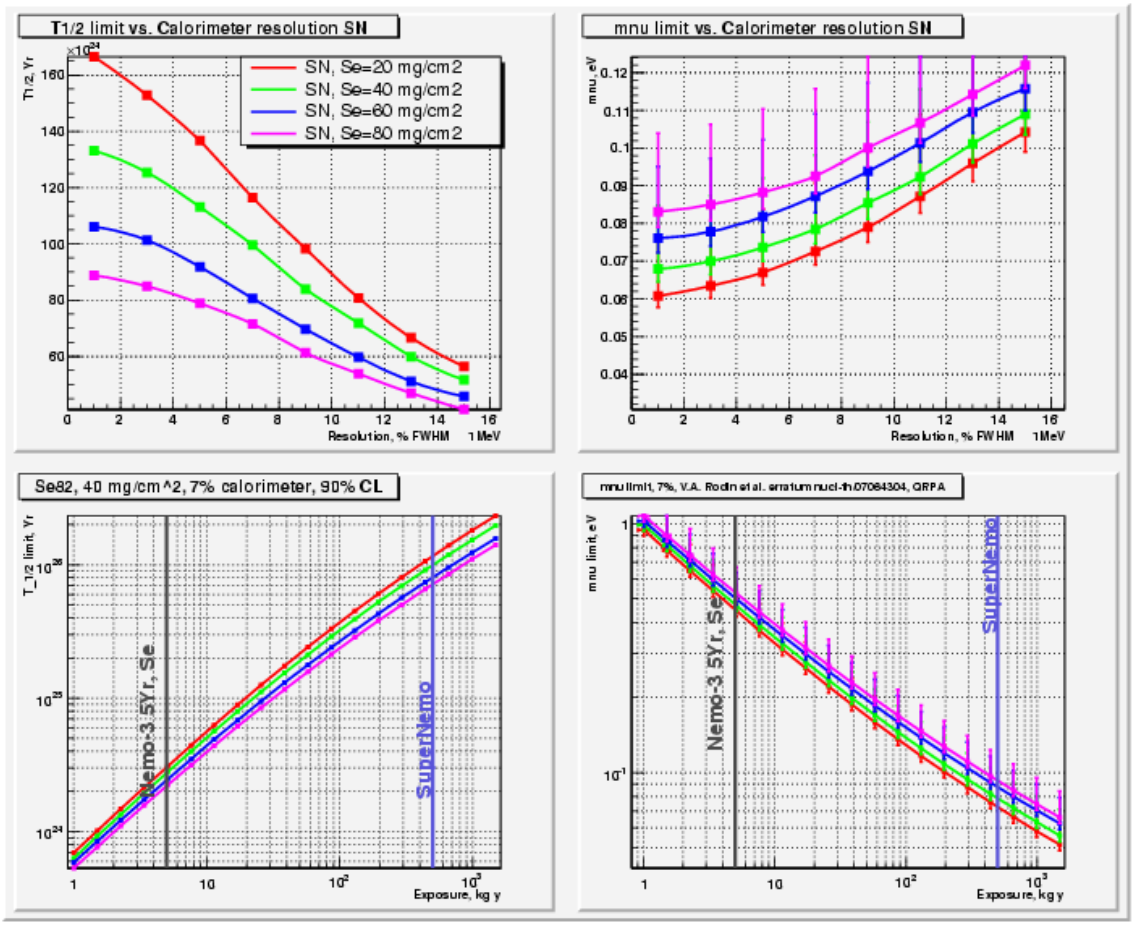


*Figure 1.6: SuperNEMO sensitivity for various source foil thicknesses. Baseline target values for source contamination are assumed (10 μBq/kg for $^{214}$Bi and 2 μBq/kg for $^{208}$Tl). Latest NME calculation is used for neutrino mass sensitivity plot.*

# 2.0 Demonstrator module design outline and dimensions.

The design of the demonstrator is based on the results of physics simulations, prototype results, NEMO-III experience and underground lab and transportation constraints. Since the decision on the LSM extension is going to be made only in 2011, the design of the Demonstrator has to take into account existing constraints of the current LSM lab where the NEMO-III detector is installed. An outline of this design accounting for the above constraints is shown in Fig 2.1.

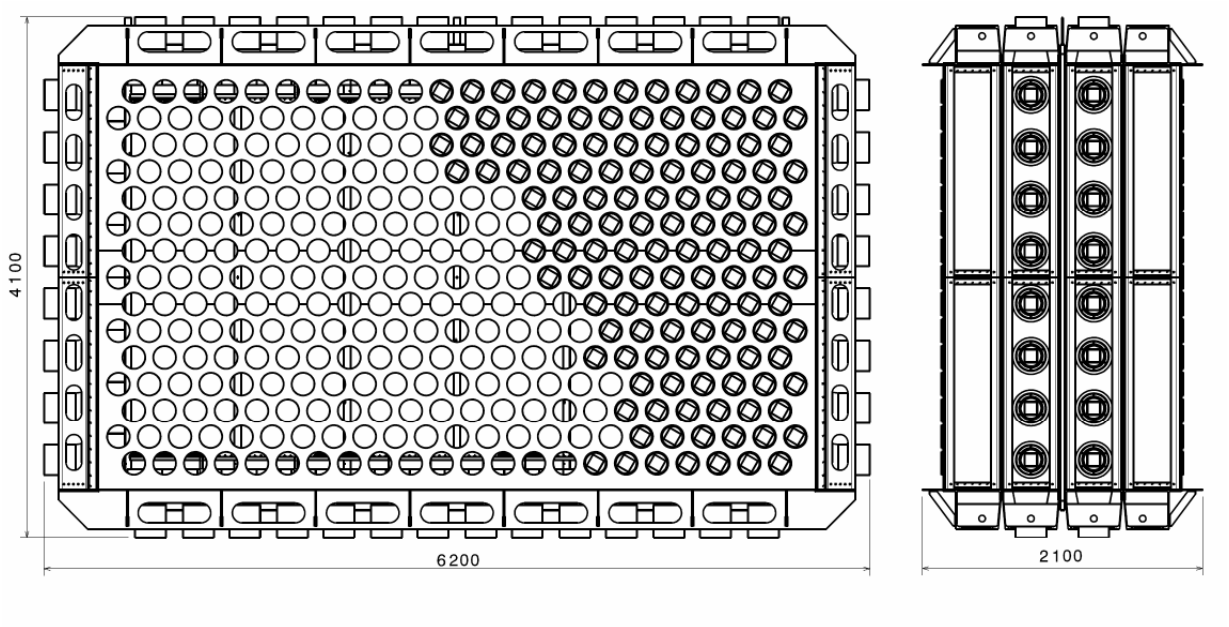


*Fig 2.1 : Conceptual design and outer dimensions of the Demonstrator module.*

The main dimensions of the module are as follows

- Height – 4.1 m
- Length – 6.2 m
- Width – 2.1 m
- Source foil dimensions – 2.7 x 4.9m (H x W) (Current Mech Proposal)-TLPH
- "Active" tracker detector height (Length of the anode wire between copper cathode rings) – 2.8 m

# 3.0 SuperNEMO Tracking detector

The SuperNEMO Tracker is essential for rejecting background and measuring the decay properties of a possible signal. It is used to reconstruct the decay vertex, to identify electrons and positrons through charge measurements if a magnetic field is present, to identify short-range alpha particles and to separate electrons and photons. During the design study phase, we have optimised the tracker parameters using simulations and several small-scale prototypes with up to 90 cells. This includes the anode and cathode wire diameters, the cell length, the wire configuration and the end cap design. The main aim of the tracker part of the Demonstrator module will be to demonstrate the capability for reliable large scale production including the wiring robot; to successfully integrate the tracker in a full detector module; to perform measurements under physics conditions.

## 3.1 Tracker cell design

The basic tracker cell design is built on the NEMO-III experience. Electrically, the unit cell has a central anode surrounded by 12 ground wires. The wires are shared with neighbouring cells to minimise their number. However, there are sizeable differences between the NEMO-III and SuperNEMO design. Mechanically, the wires of a cell are strung between two endcaps. The endcap consists of an injected moulded Delrin block, which supports the copper anode and cathode wire

terminations, together with a cylindrical copper pickup ring. The wires are individually clamped to the relevant connector by two part Delrin pins. The main reason for these design differences is due to the fact that the SuperNEMO tracking detector will be wired with an automated wiring robot. Automated wiring is a necessity for SuperNEMO due to a large number of tracker channels needed and the strict radiopurity requirements.
All wires will be made of stainless steel, which will be produced by TRAKUS-Bremicker Feindrahtwerk GmbH in Germany as a special run paying particular attention to the die quality.

The design of a basic cell is shown in Figs. 3.1a.

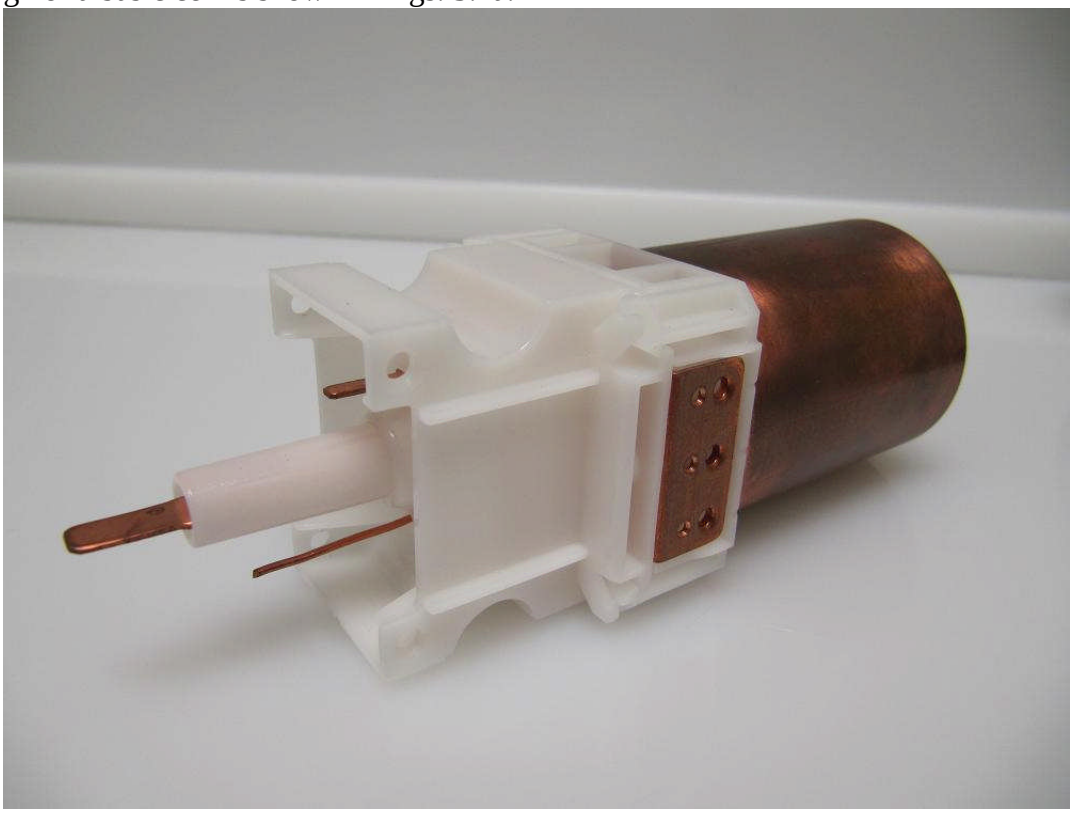

*Fig 3.1a : SuperNEMO basic tracker cell*

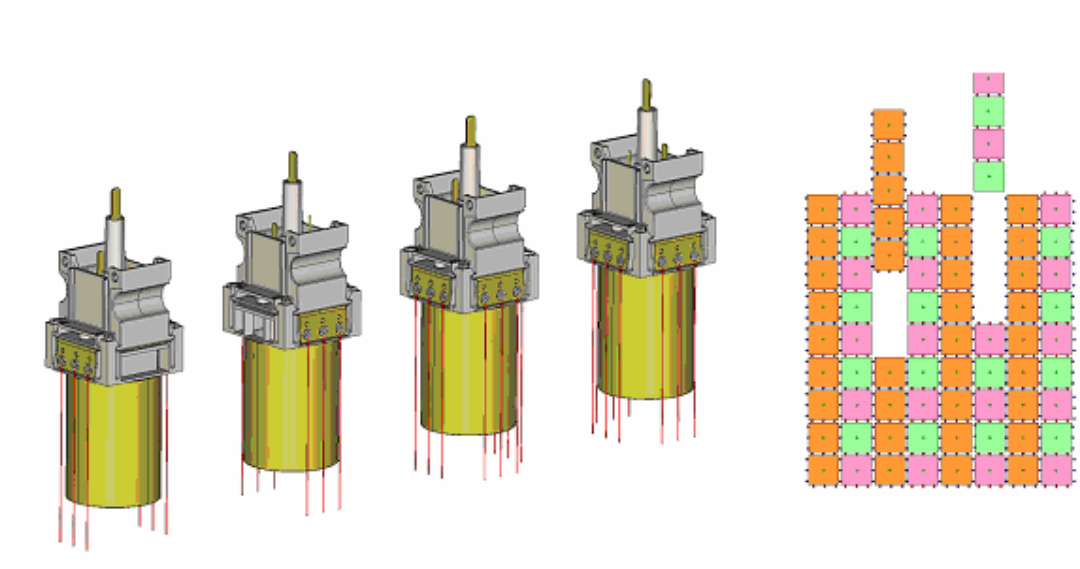

*Fig 3.1b :Endcaps showing cathode wiring options*

The individual endcap components can be configured such that the cathode wires can be strung on 1, 2 or 3 of the faces as required (Fig 3.1b). Stacking the different cell types together allows the wires to be shared between the unit cells and the cell columns, normal to the foil, to be moved as an entity.

The diameter of the anode wire is 40 µm, while the cathode wire is 50 µm. The cross section of each cell is octagonal with a diameter of 44mm (compared to 30 mm in NEMO-III ). The larger diameter of the SuperNEMO cell reduces the number of tracker channels, simplifies automated wiring procedure and allows a standard diameter of the copper tube to be used, thus reducing the cost. The performance of the new cell has been checked with the 9 and 90-cell prototypes (see section 3.2) backed up by simulations.

The cell works in the Geiger mode with a mixture of helium (95%), argon (1%) and ethyl alcohol (4%). The typical operating voltage for the anode wires is 1700-1800 V. When a charged particle crosses the cell, the ionised gas yields around six electrons per centimetre. These electrons drift towards the anode wire at a speed of 2.5 cm/µs when they are close to the anode and 1 cm/µs when they are further away in accordance with the electrical field in the cell. Measurement of the drift times (with $t_0$ defined by the calorimeter) are used to reconstruct the transverse position of the particle in the cells. The anode pulse has a fast rise time (around 10's of ns) which can be used to provide a good time reference for the TDC measurement. The avalanche near the anode wire develops into a Geiger plasma which propagates along the wire in both directions at a speed of 6-7 cm/µs depending on the working point of the Geiger plateau. The arrival of the plasma at the ends of the wires induces a signal on the cathode rings. The propagation time, measured as the time between the anode pulse leading edge and sharp signals from the cathodes, is used to reconstruct the longitudinal position of the particle as it passes through the cell. It is also possible to use the anode cell pulse shape to determine the propagation time. This however requires full digitisation of the pulse with a FADC, not just discriminator/tdc readout. In this case, only one cathode ring is necessary to resolve the top-bottom ambiguity. An example of anode and cathode pulses is shown in Fig. 3.2.

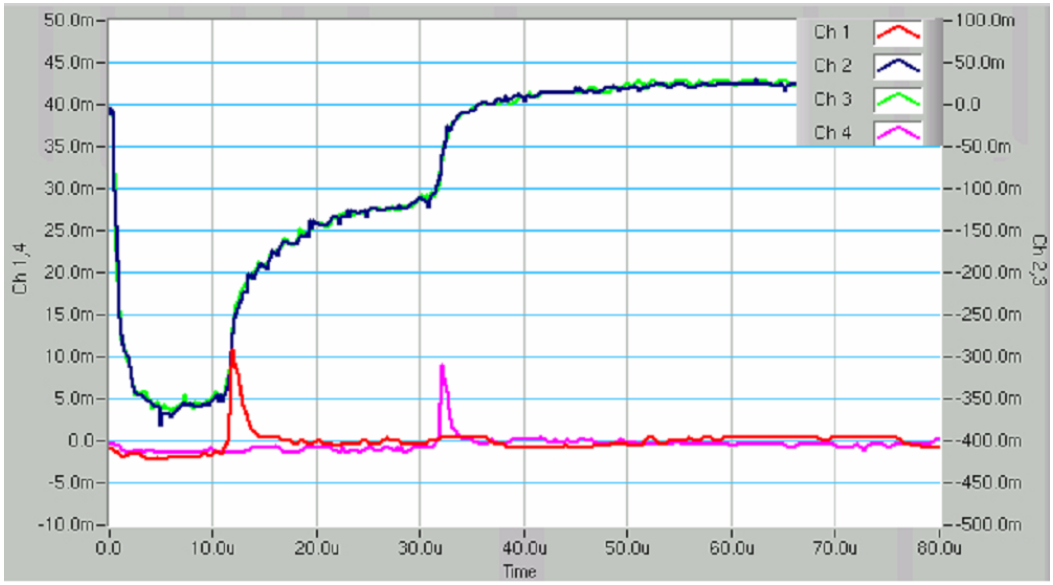


*Fig 3.2 : Anode and cathode pulses recorded from a tracker cell*

## 3.2 Tracker cells performance

The performance of the modified design of the SuperNEMO tracker cells has been extensively studied with a number of prototypes: 1-cell, 9-cell and ultimately with the 90-cell prototype. Fig 3.3 shows the 90-cell prototype installed in the University of Manchester. NEMO-III Geiger readout cards and a digital scope based readout have been used for these studies. The performance of the 90-cell tracker was assessed using cosmic ray muons. Plastic scintillator detectors above and below the 90-cell prototype have been used for triggering.

A straight line $\chi^2$ fit was used to identify the muon tracks. The information was then used to investigate key detector parameters: efficiency, drift time-distance relation, transverse and longitudinal resolution of the cells. A summary of key results is shown in table 3.1.

| Detector parameter | 90-cell results |
|---|---|
| Anode efficiency | 98% |
| Cathode efficiency | 91%* |
| Mean plasma propagation time | 52 μs |
| Transverse hit resolution, (σ) | 0.7 mm |
| Longitudinal hit resolution, (σ) | 1.3 cm |

*Table 3.1 Summary of the tracker performance obtained with the 90-cell prototype.*
**Cathode efficiency for cells without known blockages and readout problems*

Note that the length of the 90-cell prototype is 4m. Although the length of the Demonstrator tracker is 2.9 m, it is important to investigate the performance of a longer tracker which could be used for subsequent super-modules.

## 3.3 Tracker Cell Production

One of the main aims of the Demonstrator module is to set up an efficient mass production chain for automated cell production which is independent of the final tracker assembly sites. Preassembled cells can be easily transported on simple pegs. For the Demonstrator module, individual cells will be first wired in Manchester using an automated robot (see section 3.3.3). Cells are transferred to simple frames in a cassette based storage system and tested under gas and high voltage (HV) for proper Geiger plasma propagation. The test system comprising readout, HV, gas handling and cassette storage together with component cleaning will be installed in Manchester and every cell produced will be tested. Cell assemblies will then be shipped to MSSL for insertion and integration into the main tracker frame.

### 3.3.1 Radio purity and Cleanliness of components

Building on NEMO-III experience, the tracker design utilises known acceptable low background substances such as Delrin for the endcap mouldings and OHFC copper for the conductors. Raw materials will be sampled and undergo detailed low background measurements before moving to the production phase. Similarly, finished components will be checked. Radiopurity measurements include gamma spectrometry with ultra-low background HPGe detectors and Rn emanation studies with purpose built detectors. See section 7 for more details on the detectors and procedures and sensitivities for different materials.

Apart from radio purity considerations, cleanliness, particularly of the wire and cell components, is essential for proper Geiger operation. Automated wiring is therefore needed to minimise human contact. Cell assembly and testing will take place in the Manchester clean room. The wiring robot itself will be equipped with an additional laminar flow curtain to achieve conditions approaching class 100 in the vicinity of the cells. Components will be ultrasonically cleaned, and copper components will undergo a final surface etch to minimise contamination. Nitrogen purged clean storage cabinets will also be used.
A database and bar coding system will be set up to keep track of component history.

### 3.3.2 Wire

Propagation of the Geiger plasma along the 40 micron stainless steel anode wire has been shown to be sensitive to imperfections of the wire surface. As in NEMO-III, the wire will be produced as a special run by TRAKUS-Bremicker Feindrahtwerk GmbH in Germany, paying particular attention to the die quality. Following detailed discussions with Trakus, steel from two sources will be put aside for the Demonstrator Module. 1 kg samples of each will then be tested for radio purity. If acceptable, the steel will then be drawn to size and, after cleaning, a further sample will be measured.
A cleaning station will be built, mainly from commercial units, in which the wire will be cleaned with heptane as it is run onto spools for use in the wiring robot. The anode wire will undergo an additional step, where it will be heat treated at a temperature of ~200ºC.
.

### 3.3.3 Wiring Robot

A working prototype of the wiring robot installed in the Nu-Lab at MSSL is shown in Fig. 3.3

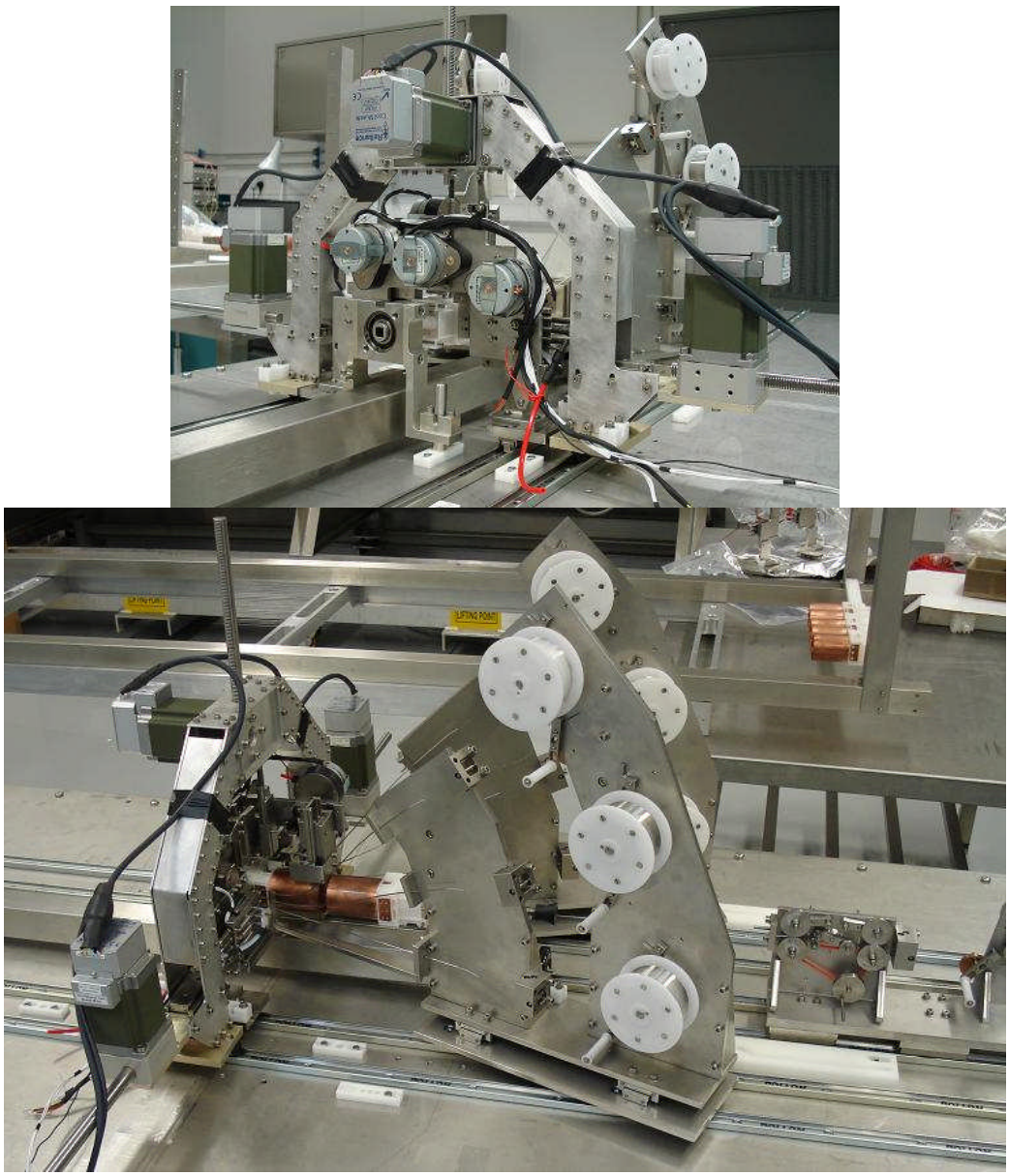

*Fig 3.3 : Wiring robot*

The key components of the wiring robot are described below.

- *Clamp pin feeder:* This mechanism will orientate and pre-assemble the two part clamp pin, then present up to ten of these assemblies (one for each of the 9 cathodes and 1 anode) to the pick and place tools for loading onto the Clamp Pin Inserter Mechanism.

- *Pick and Place Tools:* Pick and place tools will take the clamp pins from a storage area on the wiring robot and load the pins into the Clamp Inserter Mechanism. This system will ensure that the pins are inserted in the correct orientation prior to wiring.

- *Clamp/Cutter for First Wired Cell:* This system will thread, guide, clamp and cut up to ten wires on the first end cell, thus allowing the cell to be "drawn" out to the required length. These operations happen in a defined sequence and require feedback at each stage to ensure that different parts of the mechanism are operating correctly.

- *Clamp/Cutter for Second Wired Cell:* This system will guide, clamp and cut the wires at the other end of the cell ensuring that all wires are terminated cleanly with the correct tension applied.

- *Actuator Mechanism:* This system needs to be developed further from its current state and the control system for the stepper motor actuation refined and tested. This system supplies the necessary mechanical force to insert up to 6 pins simultaneously. In addition, the assembly will require sensors and alignment devices to allow the system to be electronically driven to the required positions on the robot table.

- *Electronic Positioning System:* This sub-system will move all of the mechanisms on the robot table. It will require feedback sensors and end stops to ensure correct system alignment at each phase. The actuator and clamp/cutter mechanisms need to be traversed along the table in sequence as each action is performed to repeatable positions. This system includes the necessary electronics for drawing out the cell to the required length and rotating the cell in order to present the correct orientation to the wiring robot.

- *Electronic Wire Feeding and Tensioning:* Only the anode wire needs to be mechanically fed. The feeding mechanism has been tested satisfactorily during the 90-cell prototype assembly. The system now requires electronic drives and feedback sensors to automate the system. All of the seven wire spool assemblies require motor drives to allow them to be driven backwards for wire tensioning. The wire is tensioned by weighted arms, which are raised, providing a calibrated tension. When the arms reach this position, a sensor is activated and a signal is fed back to the motor drive to hold position. The wire is then held at the required tension during the clamping operation and released prior to cutting.

- *Robot Table:* The robot table provides a repeatable reference plane for the mechanisms to operate from. This is achieved by modifying/replacing/extending the existing assembly with aluminium tooling plate and adding a set pattern of pre-drilled/threaded holes. The implementation of a set pattern of holes will allow systems to be simply bolted to the table as required.

- *Cell Transfer system:* End caps need to be loaded on and off the table automatically to reduce human interference. The loading system is likely to be a magazine system which will hold up to a day's worth of cells. The cells will then be transferred onto a support frame before being inserted into the test tank.

- *Control System:* Manchester is developing the control system for the robot. A scalable modular drive system has been identified for the 20 or so motors required, together with I/O cards for the various position sensors, micro-switches etc. Labview software is being written for these functions. As the individual mechanisms discussed above are finalised, the relevant drive modules will be implemented. Once individual mechanisms have thus been commissioned, the overall sequencing software will be added, together with test measurement systems such as wire resistance and wire tension.

The wiring robot will be transferred to Manchester where the cells for the Demonstrator module will be wired.

### 3.3.4 Cell Inspection and Testing

Simple initial inspection tests will take place automatically on the robot, such as electrical continuity and wire tension - primarily to ensure the mechanical integrity of the wire terminations. Cameras will be used to view wire clamps etc. remotely. The wired cell will then be transferred to pegs within a clean storage cassette mounted adjacent to the robot.

A cassette of cells, corresponding to about a day's production will be transferred to a segmented gas tank, flushed with gas for an appropriate time, and powered. After a short high voltage soak test, a readout system (a variant of that used for the current 90 cell prototype) will employ a cosmic trigger to verify that full plasma propagation occurs along each wire (i.e. there are no wire defects or dust) and other characteristics of the cells: anode and cathode efficiencies.
Considerable thought and effort has gone into the design of the cell endcaps and the cassettes, so that a tested sub-unit consists of a complete column of (9) cells, which are normal to the foil. This will ensure that, once delivered to MSSL, the sub-unit can be pushed directly from its storage cassette into the main frame minimising cell handling.

A major challenge is to minimise the 'transit time' of a cassette, both to get reasonably fast feedback of potential faults and to simplify the logistics of multiple detectors under test. A certain time will be needed to reach the correct gas concentration, and further time for a high voltage soak test, whilst actual data taking is relatively fast.

The detector gas of the SuperNEMO tracker used in the test module is 95% helium, 1% argon and 4% ethanol. As each day's production corresponds to a volume of about 300 litres, gas handling will be optimised. The current plan is to have a stack of four stages. Gas flows 'backwards' through the stages in series i.e. in at the 'oldest' cassette which is taking the data, then flushing the previous stages. The gas system will also have to purge incoming cassettes to remove air and outgoing cassettes with nitrogen to remove chamber gas for storage.
Since cell components are relatively cheap, any faulty cells will be abandoned rather than repaired. We are aiming for this to be at the 1% level or better.
The existing 9 and 90-cell test tank setups will remain available if fault studies are required.

### 3.3.5 Transport

Tested cells are removed from the gas system in their clean cassette, which is then purged with dry nitrogen and sealed in a cleanroom bag. Sealed cassettes will be packed into a clean transport box and sent to MSSL by road. Typically deliveries would be weekly or fortnightly corresponding to 100 – 200 cells. Empty cassettes are recycled by the next run. Sufficient cassettes and clean storage space are required to provide a buffer to decouple potential delays at either end.

### 3.3.6 Tracker frame and Assembly at Nu-lab

The overall tracker frame is designed and constructed by MSSL, in consultation with the LAL engineers. The basic material for the frame is stainless steel and iron sourced from manufacturers known to produce low background material.

The tracker module will be split into 4 C-shaped sub-modules. Two C-shaped sub-modules join together to form a tracker sub-module on one side of the source foil module. The sub-module dimensions are dictated by transport and access considerations. These are height 4.1m, length 6.2m and width ~0.5m .
Each section of tracker will be assembled and sealed for Radon emanation testing (see section 7.3). Four sections of the tracker will be assembled at MSSL with all cells inserted and connected to the electrical feedthroughs.

The cells are arranged in columns, which are inserted perpendicular to the source foil. The cell layout has been redesigned to allow complete columns to be inserted or removed at any time during the assembly process. This is achieved using cells with different cathode wire arrangements to ensure that there is no mechanical interference between cells in adjacent columns. The cells are supported on an insertion frame, which is lifted into position to transfer the cells. All of the cells in each column are electrically and mechanically connected onto a single connector block which interfaces with the electrical feedthrough via a bespoke radio-pure connector.
If a fault is found with a particular cell, the column containing this cell can be removed from the tracker and replaced. It is foreseen that this operation could also be carried out in the final Demonstrator via the removal of the calorimeter wall.

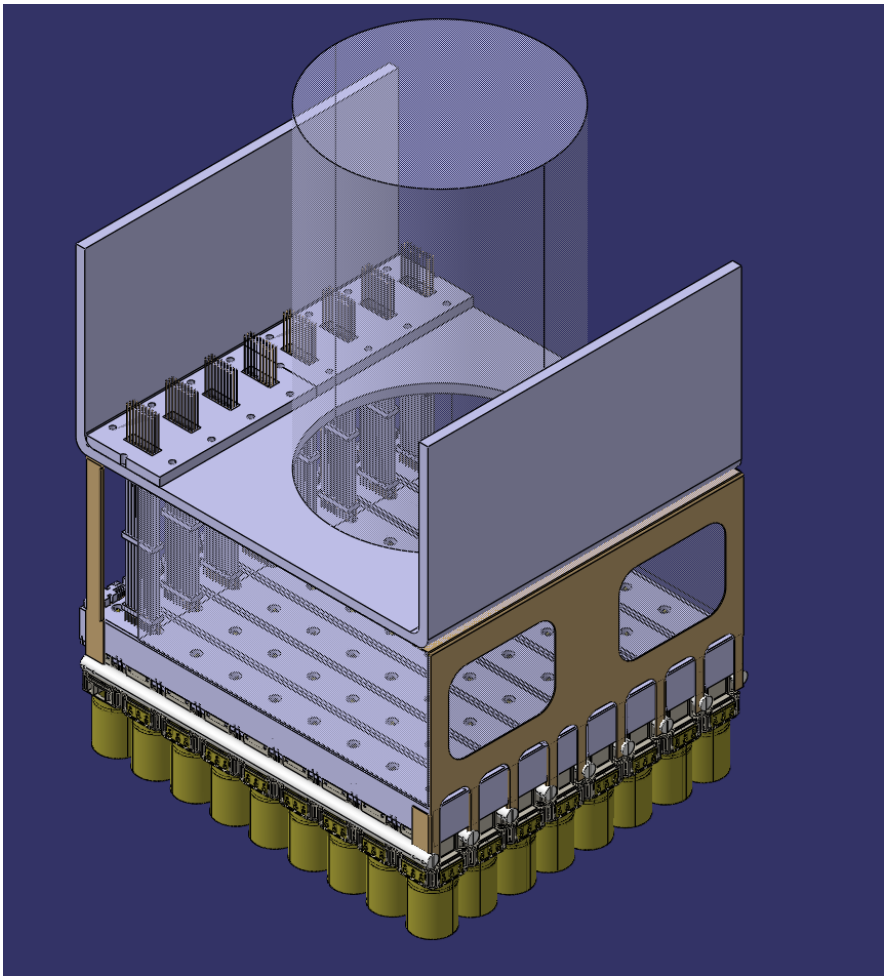

*Fig 3.4 Cell Support Frame Conceptual Design*

Figure 3.4 shows the columns of nine cells, which are inserted from the far side where the calorimeter is to be attached. The cell support frame is arranged around the gamma tagging scintillator block and is constructed from copper and delrin.

Tested cells will be shipped from Manchester inside clean cassettes at a rate of about 100 per week. Blocks of cells will be moved from the storage cassettes and installed into the sub-module frame, using a cell support frame. Cable service looms (HV and signal) are installed and feedthroughs sealed. Continuity and resistance tests will be carried out to ensure cell wires are still connected correctly after transportation. UV inspection will be utilised to remove any contamination which may have been introduced during cell transferral.
It will not be possible to test the cells again under gas until a section (1C section) of the tracker is complete. Gas sealing for these sections can be achieved relatively easily. However, it is not

practical to test cells again on a weekly basis due to complications of reconfigurable gas volumes and required times to reapply the gas.
During integration, cells will be covered with clean mylar to keep contamination to a minimum.
Initial functionality tests at the sub-module level will use readout systems based on the NEMO-III Geiger readout cards. Module sectors in turn will be powered and tested to check simple cell functionality using a cosmic trigger. If required, individual cells could be replaced at this stage.
On this timescale, NEMO-III itself will be being decommissioned and NEMO-III readout cards and associated hardware will be available.
Completed sub-modules will be rotated to the vertical and joined to form the complete tracker. A copper dummy source foil will be used for commissioning tests. The top and bottom part of the tracker frame will be equipped with plastic scintillator produced in Dubna and NEMO-III PMTs, which will act as a veto to reject SuperNEMO background events. The veto blocks will also be used for triggering during commissioning at the Nu-Lab.

### 3.3.7 Feedthroughs

The tracker module requires a large number of high voltage electrical feedthroughs for the Geiger cells. Each connection requires a number of breaks in the signal line to allow for easy assembly/disassembly and maintenance. Off the shelf components are available for these applications. However, with large numbers of components, the mass of material becomes significant with radiopurity being the most significant issue. It is therefore proposed that the bespoke feedthrough is constructed using known radio pure materials. This is a challenging piece of work as the design must be gas tight for helium and be safe for use up to 1800-2000 volts. The current conceptual design is looking at using delrin insulated copper components which will form plugs and sockets. Gas tightness will be achieved by directly potting the copper wires into a hole in a feedthrough plate. The adhesive has been identified and tests will be underway early in the programme, so that alternatives can be sourced if necessary.

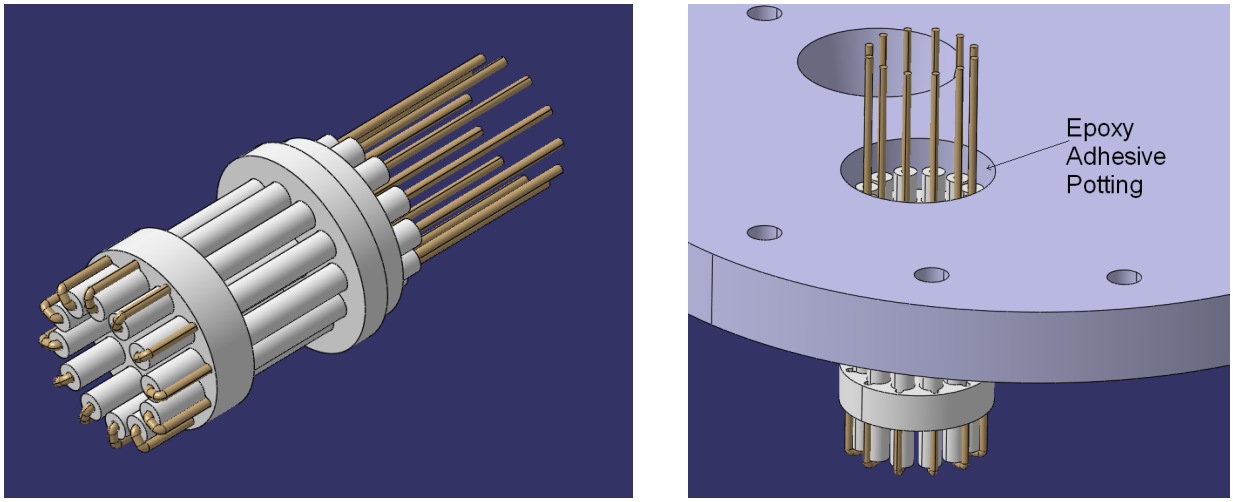


*Fig 3.5 Conceptual HV feedthrough test design*

# 4.0 SuperNEMO Calorimeter

The three main functions of the SuperNEMO calorimeter are to measure the particle energy, to make time-of-flight (TOF) measurements to reject and measure external background and to give a

fast trigger signal. The Demonstrator module will have 550 calorimeter blocks on the walls and 32 veto blocks on top and bottom of the tracker module.

## 4.1 Basic calorimeter block

One of the most challenging tasks faced by SuperNEMO is to reach the calorimeter energy resolution of 7-8% FWHM at 1 MeV, unprecedented for this type of detectors. Feasibility to reach this resolution with a large baseline design block has been demonstrated during the design study [9]. However, this resolution was reached for several blocks developed in laboratory conditions. The main goal now is to show that it can be maintained during mass production of hundreds and thousands of scintillator blocks and PMTs. This is one of the main goals of the Demonstrator module. In addition, it will address the issue of the calorimeter components radiopurity, most importantly the PMTs which are the main source of the external background in SuperNEMO.

A single calorimeter block is comprised of a plastic scintillator block coupled to a low radioactive PMT. The plastic scintillator has been chosen to minimise backscattering of low energy electrons for their radiopurity. The scintillator block has a hexagonal shape with a diameter of 27 cm on the side facing the tracking detector and a concave surface on the opposite side matching a hemispherical shape of an 8” PMT. This arrangement avoids the necessity of a light guide to couple the PMT to the scintillator block and maximises the light collection and hence provides the optimum energy and time resolution. An example of basic calorimeter block is shown in Fig. 4.1

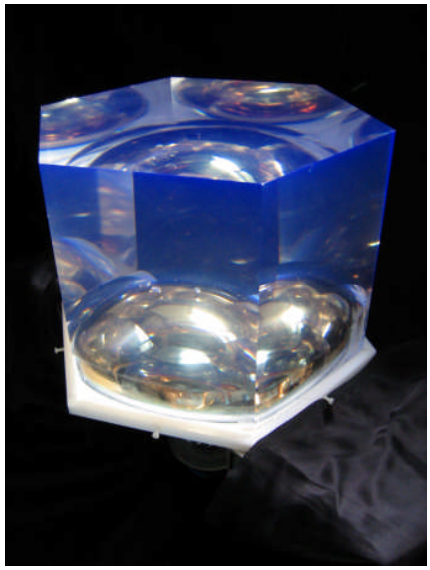

*Fig. 4.1 SuperNEMO calorimeter block*

The scintillator material used for the calorimeter wall is Eljen EJ-200. The photo-detector is a super-bialkali 8 inch hemispherical PMT produced by Hamamatsu, R5912-MOD. This PMT was developed in close collaboration between SuperNEMO and Hamamatsu. It has 8 dynode stages which provides an excellent linearity up to very high light levels necessary to obtain the required

energy resolution of FWHM = (7-8)%/√E(MeV). The PMTs will be produced using low background glass and other components.
Final details of the design of the SuperNEMO calorimeter block are being worked on by the CENBG group with input from other groups involved in the calorimeter development.
The top and bottom veto calorimeter blocks are not used for ββ event selection but only for tagging gammas from background events. Polystyrene scintillator produced in Dubna and NEMO-III PMTs will be used for these veto counters.

## 4.2 PMT and scintillator specifications and procurement

Work on defining specifications for the PMTs scintillators is ongoing and concentrated in CENBG. This work is carried out in close contact with manufacturers. A document is being prepared which will form the basis of the purchase order. A QA procedure will be set up where the main specifications will be defined. These will include

- Radiopurity of PMTs.
- QE of PMTs.
- Uniformity of photocathode.
- Linearity of PMT.
- Dark current and noise.
- PMT gain (with standard divider base) and stability.
- Nominal light output of scintillator translated into energy and time resolution.
- Emission spectra of scintillator.
- Polishing quality of scintillator block.
- Uniformity of scintillator block

## 4.3 Assembly and characterisation

The procedure is being developed by CENBG and other groups.

## 4.4 Calorimeter calibration

The purpose of the calibration system is three-fold: to convert the digitised pulse height and time data into absolute energy and time units (e.g. MeV and ns); to provide regular corrections for possible gain drift of the calorimeter modules; to map out the linearity of the calorimeter response. The first task is addressed by radioactive sources emitting electrons and gammas. A light injection system is used to calibrate the gain and linearity. In addition, a subset of the calorimeter modules will be equipped with a low activity alpha-sources embedded into scintillator to cross-check the gain calibration provided by the light injection system.

### 4.4.1 Absolute calibration

In order to provide an absolute calibration (ADC-energy conversion), Bi207 radioactive sources will be used and periodically inserted into the apparatus in well-defined positions. The Bi207 decay provides conversion electrons with energies of 482 keV, 976 keV and 1682 keV (K-lines, with the last line having very low branching ratio and therefore not used under normal conditions of the calibration runs). The Demonstrator module will be equipped with copper tubes running along the edge of the source foil. An automatic system for the delivery and withdrawal of the calibration

source will be employed. 15-20 Bi207 sources will be used in the Demonstrator module to cover all calorimeter blocks with adequate statistics over a 24 hr calibration time. Most of the Bi207 decays result in γ-rays, thus the tracking chamber must be in operation to select electrons originating from the calibrations source positions. This limits the activity of the sources which is on average ~200 Bq.
To cover realistic energies emitted in the double beta decay process, additional sources of Sr90 will be used which provide higher electron energies. Y90, the daughter of Sr90, is a pure electron emitter with the end-point of β-spectrum of 2.28 MeV. This calibration does not require pattern recognition with the tracking chamber because the events of interest are located in the tail of the spectrum, which can only contain electrons coming directly from the source position. Thus, relatively intense sources and shorter runs can be used.
Timing information is used to discriminate between external and internal events for background studies and rejection. The timing offsets for each of the calorimeter modules will be determined using two coincident γ-rays with energies 1332 and 1173 keV emitted by a Co60 source.

The current plan is to perform the Bi207/Sr90 calibration every two-three months and the Co-60 calibration once a year. The required frequency of absolute calibrations will be determined by the performance of the Demonstrator detector.

### 4.4.2 Gain and linearity calibration

The gain calibration is a very important and challenging task. An unaccounted gain variation produces a similar effect to that of a poor energy resolution, with energy distribution of double beta and background events "washed out" resulting in background events falling into the energy window of interest. To reach the target sensitivity of $10^{26}$ yr with a calorimeter energy resolution of (7-8)%/√E(MeV), we need to control the gain at a 1% level. From NEMO-III experience, we know that it is a very challenging task. Therefore the Demonstrator module will be equipped with a redundant gain calibration system based on the light injection system and low activity alpha sources embedded in some of the scintillator blocks. The choice of the final SuperNEMO calibration system will be made based on the Demonstrator performance.

### 4.4.3 Light injection calibration system

The light injection (LI) calibration system is based on UV LEDs with a peak wavelength in the emission spectrum of 390 nm injecting light into calorimeter blocks through clear fibres. The choice of the LEDs is a compromise between the cost and performance (390nm light does excite the plastic scintillator). The fact that the light is injected into the scintillator rather than directly in the PMT is an important feature of the design:

- The dependence of the LED wavelength emission spectrum on the light level determined by the amplitude and width of the LED driving pulse is avoided.
- The LI events have the same wavelength as the real events from ionising radiation.

To avoid the tail of the LED emission spectrum getting through to the PMT a wavelength dependent filter is used. The LED light level is monitored using dedicated monitor PMTs which receive the light from separate fibres and are equipped with Bi207 sources to survey the gain of the monitor PMTs. In addition, photon statistics is used to estimate the number of photo-electrons produced at the photo-cathode according to the formula:

$$NPE = (Q/\sigma)^2 \, (1+1/g_1)$$

where $Q$ and $\sigma$ are the mean and RMS of the ADC pulse height distribution and $g_1$ is a secondary emission ratio (the gain of the first dynode) determined from a single photo-electron fit.

The gain survey will be performed twice a day by injecting a certain amount of light from LEDs. Once every three months, linearity curves will be taken. The procedure will involve the injection of different light levels to map out the linearity of the calorimeter response.

The required energy resolution of SuperNEMO leads to very high light levels that the PMTs will operate at. More specifically, 1 MeV corresponds to 1000 pe produced at the photo-cathode. At these light levels, significant non-linearities are expected from standard PMTs due to a space-charge effect between the anode and the last dynode. To address this issue, an 8 dynode stage tube has been developed by Hamamatsu in collaboration with SuperNEMO. It has a lower gain but much better linearity characteristics. Fig. 4.2 shows a linearity curve obtained with a R5912-MOD tube. The plot shows less than 1% deviation from linearity at ~3700 NPE (corresponding to ~3.7 MeV) and is in good agreement with expectations from Hamamatsu for this tube.

The LED will be hosted in a custom-made pulser box that will provide the circuitry for driving LEDs and a system for light distribution between the fibres. The design of the pulser box and the light distribution system will be based on the design developed for the LI system of the MINOS experiment with necessary modifications taking into account the light level, wavelengths and uniformity required by SuperNEMO.
The fibres will be connected to the scintillator blocks using the following procedure. A short length of 1mm clear optical fibre is glued using optical cement BC600 in a hole pre-drilled at the back of the scintillator block. The fibre will have a commercial SMA connector which has a transmission at the required wavelengths of >95%. A matching SMA connector will be at one end of a long fibre running to the pulser box where LEDs are hosted. A schematic of the fibre connections is shown in Fig 4.3.

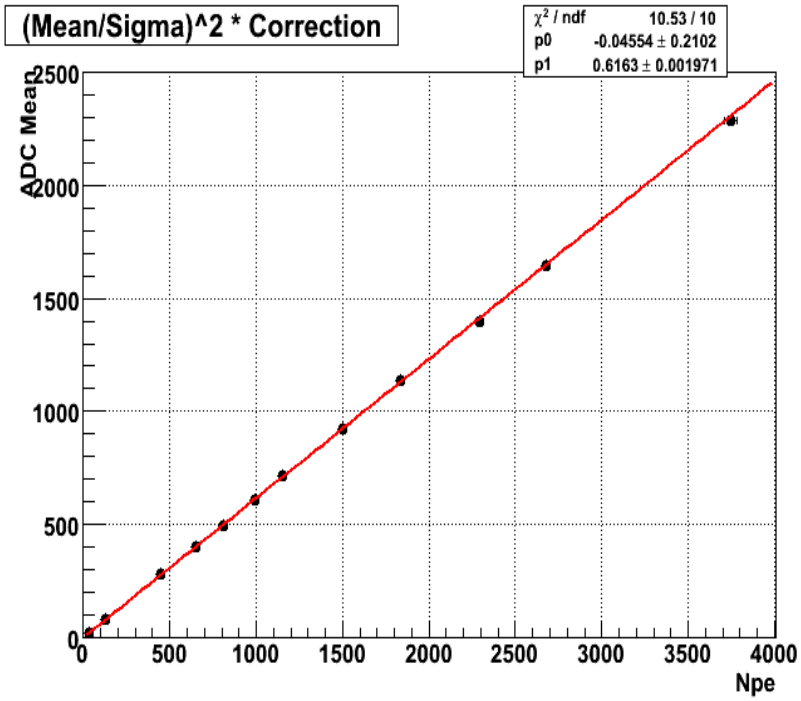


*Fig 4.2 Linearity measurement of the Hamamtsu R5912-MOD at 1900V (corresponding to a gain of $7\times10^5$) showing less than 1% deviation from linearity at ~3700 NPE (~3.7 MeV)*

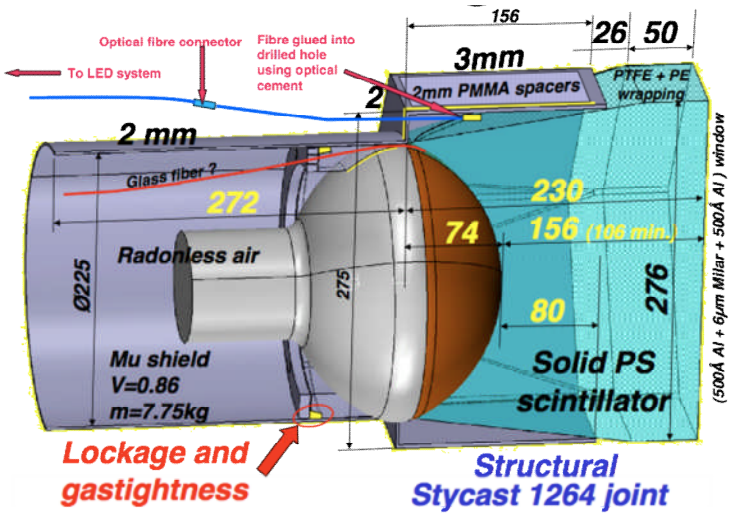


*Fig 4.3. A schematic of the LI calibration fibre connection to a SuperNEMO scintillator block.*

.

### 4.4.4 Gain calibration with alpha sources

A subset of the calorimeter scintillator blocks will be equipped with low activity alpha sources embedded in the scintillator. The two main sources under consideration are Gd148 ($E\alpha$ = 3.27 MeV, $T_{1/2}$ = 74.6 yr) and a "light source" based on Pu238 ($E\alpha$ = 5.5 MeV, $T_{1/2}$ = 87.7 yr) embedded in the non-organic scintillator $YAlO_3$:Ce. The quenching factor of the plastic scintillator is ~10% meaning Gd148 will give a reference point at ~330 keV. The light source will give a reference point at ~2 MeV. The activity of the alpha sources will be at the level of 2 Bq and therefore will have to be specially manufactured for SuperNEMO.

The advantage of this method of the gain control is the stability offered by the long-lived radioactive sources. The Demonstrator module will be equipped with such a redundant calibration system in order to understand if the alpha calibration system is needed for SuperNEMO to reach the target of 1% calibration.

## 4.5 Alternative calorimeter layout (bar design).

In parallel with the baseline design, an alternative design has been investigated. It is based on long (2 m) scintillator bars read out from both ends by two 3" PMTs. In this case, the detector is split into much bigger super-modules (between 3 and 6 to host 100 kg of isotope) with calorimeter walls and source foils "sandwiched" between each other (Figure 4.4). The energy resolution with the bars will inevitably be worse than with the block design. However this might be compensated by a better background rejection (due to self-shielding) and lower overall background due to a lower PMT mass. The bar design will have a smaller number of calorimeter channels and, as a result, is cheaper.

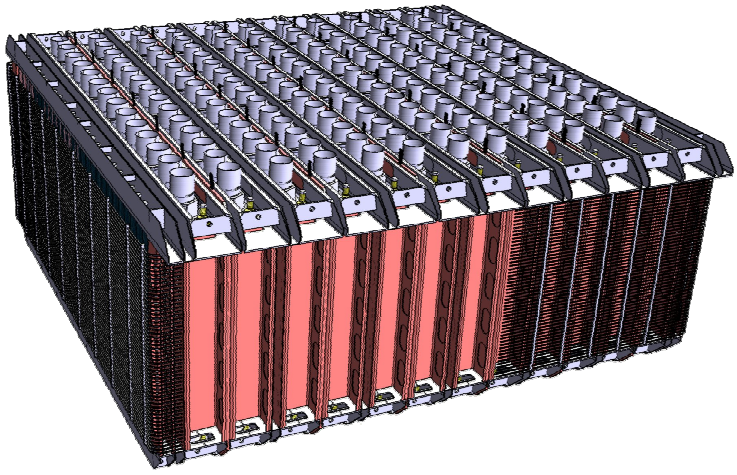

*Fig 4.4. A SuperNEMO super-module based on the calorimeter bar design.*

Extensive test bench studies have been carried out using EJ-200 (PVT) scintillator plastic bars with a dimension of 2m (length) x 10cm (width) x 2.5cm (thickness). The width of the bar is tapered to 6.5 cm to match the active photo-cathode area of the HAMATSU high-QE (35% at maximum wavelength) 3" PMT, R6233-100, attached to either end of the bar. Other bar dimensions have also been investigated. The energy and time resolution have been evaluated using two methods: by irradiating the bar with a Bi207 radioactive source and looking at the spectra of conversion electrons; and by exposing the bar to a low energy electron beam from a Sr90 magnetic spectrometer. Both methods yield consistent results. The energy resolution obtained for bars is shown in Fig. 4.5 as a function of the ionisation location along the length of the bar. The average energy resolution is FWHM = 10% and the time resolution is $\sigma$ = 450 ps (both values are at 1 MeV). These are the best results achieved for scintillator detectors of this size. However, as expected, the values are worse compared to the block design which are 7% and 250ps (extrapolated from NEMO-3 data) for the energy and time resolution respectively.

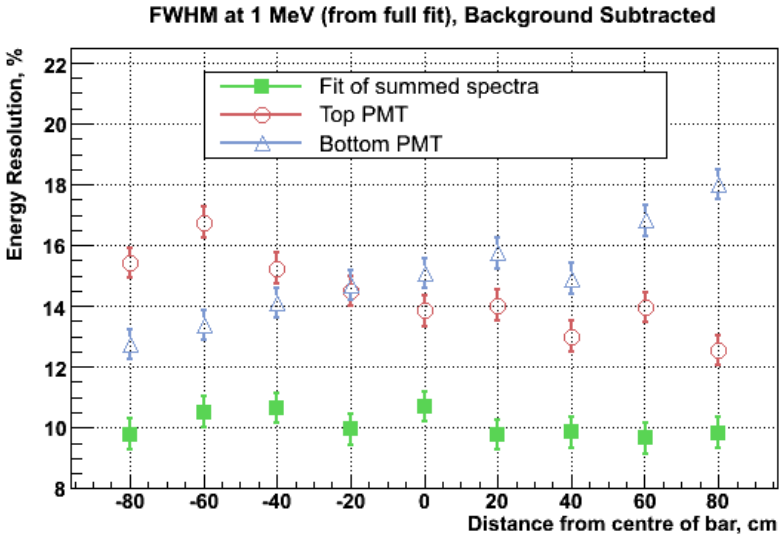


*Fig 4.5 The bar energy resolution as a function of the ionisation location along the length of the bar. The average resolution is 10% (FWHM at 1 MeV).*

The SuperNEMO Technical Board met on 3 February 2010 to consider the two designs based on the available information from simulations and test benches. It was noted that, providing the target backgrounds are reached with the Demonstrator, the block option of the Demonstrator gives a more straightforward answer to the question of the SuperNEMO sensitivity, and ultimately the sensitivity

with the block design is 50% better (half-life) with the target backgrounds. The bar design of the calorimeter has more "unknowns" due to insufficient information available for time calibration, internal/external background measurement (especially for Tl208), sensitivity to excited states.
It has been decided to proceed with the block design for the Demonstrator.

It was noted that, if the block-based Demonstrator will turn out to be limited by the PMT background, a case can be made to proceed with building a bar-based super-module housing ~15-20 kg of isotope. This approach can test experimentally the bar design and at the same time maintain the continuity of the physics programme. The bar design is therefore a backup option for SuperNEMO and the final detector design will depend on the results obtained with the Demonstrator.

# 5.0 Readout electronics and data acquisition system

The SuperNEMO detector will have independent readout electronics for the tracking and calorimeter detectors with a trigger and data acquisition system which can be inter-dependent. Its purpose is not only the triggering and data collection for ββ runs but also for calibration runs and background studies.

## 5.1 Overview of the SuperNEMO Readout

Because of the low data taking rate, it is practical to run SuperNEMO readout as a triggerless system. All significant data is recorded and time-stamped. Full events are formed by combining these data fragments offline.

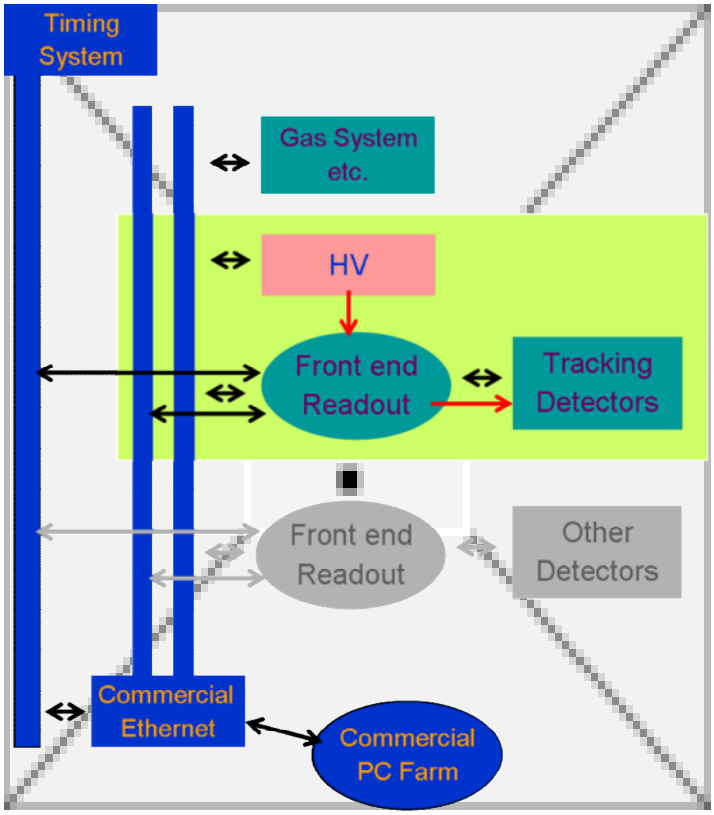


*Fig 5.1 Overview of the SuperNEMO Readout.*

Fig. 5.1 shows how the overall readout is assembled. Each detector is split into a number of independent readout sub-modules that connect to redundant Ethernet backbones built from commercial switches. The connections will be gigabit links, though 100 Mbit would be adequate for the anticipated modularity even with calibration data rates. Although the overall readout system is large, most of that scale is accommodated within the commercial (and low cost) Ethernet. There is no requirement for the multiple stages of readout buffering or triggering as might be needed in a traditional high rate particle physics experiment.

A centralized timing system will distribute a global clock and associated command data. The connection will be some differential signalling standard (LVDS, PECL, CML etc) with a 40Mhz clock being used to lock a PLL at each sub-module to provide a local clock at up to 160Mhz which runs in time with the central clock. Synchronisation and other timing critical commands will be sent over a serial link on the same physical connection as the clock (twisted pair).

The downstream data collection is performed by standard low cost commercial PC/server computers. These combine event fragments into events, log data, and perform monitoring tasks. These computing resources need not be localized at the detector.

## 5.2 SuperNEMO Tracker readout requirements

The SuperNEMO tracker cell design is an evolution of the NEMO-III cell, and as such is a mature technology. The transverse coordinate is determined by the initial arrival time of the ionization that drifts from the struck region within the 44mm cell. At small distances, the drift times vary proportionally with distance. At longer distances and particularly out near the corners of the cells, the distribution becomes non-linear, but monotonic and easily recovered offline. The longitudinal coordinate is determined by the propagation time of the Geiger discharge, which is detected by copper cathode rings at the ends of the cell acting as ‘instrumented earths’.

The readout system needs to be able to record times from the arrival at the anode and subsequent pulses seen on the cathode rings, no pulse height or other analogue information is required. A timing bin size of 12.5 ns, corresponding to an 80MHz clock, is considered more than adequate for the anode pulse and significantly more accurate than needed for the longitudinal measurement. A 40Mhz clock may also be adequate. In principle, the signals from the cathode rings are redundant and only one pulse is needed to calculate the position along the wire. For logistical reasons, we would prefer to instrument the upper ring only, but in case of some failure of the plasma propagation it would be very useful to have an alternative measurement. The anode pulse shows the structure of the extended discharge, so that the signal could be used to recover longitudinal timing, albeit with an inherent ambiguity between ends. Processing of the anode signal combined with the upper ring will give us the timing necessary to reconstruct the longitudinal position. The Demonstrator will be used to understand the cathode efficiency on a large scale. It therefore will be equipped with both cathode rings and the decision on whether to use a single (upper) cathode ring will be made based on the Demonstrator performance.

A major constraint to the design of the readout system is one of cost. A final build of around 40K channels can only be realistic if we can keep the total readout costs to less than ~50 pounds per channel.

## 5.3 Tracker Readout

The sub-module of the tracking readout is a collection of readout cards housed in a custom crate with an interface module providing connection to the Ethernet and timing system. Each readout card will handle a number of cells, 8 or 16. Each crate needs a small number of HV channels, either from a local supply, or from a centralized commercial HV supply.

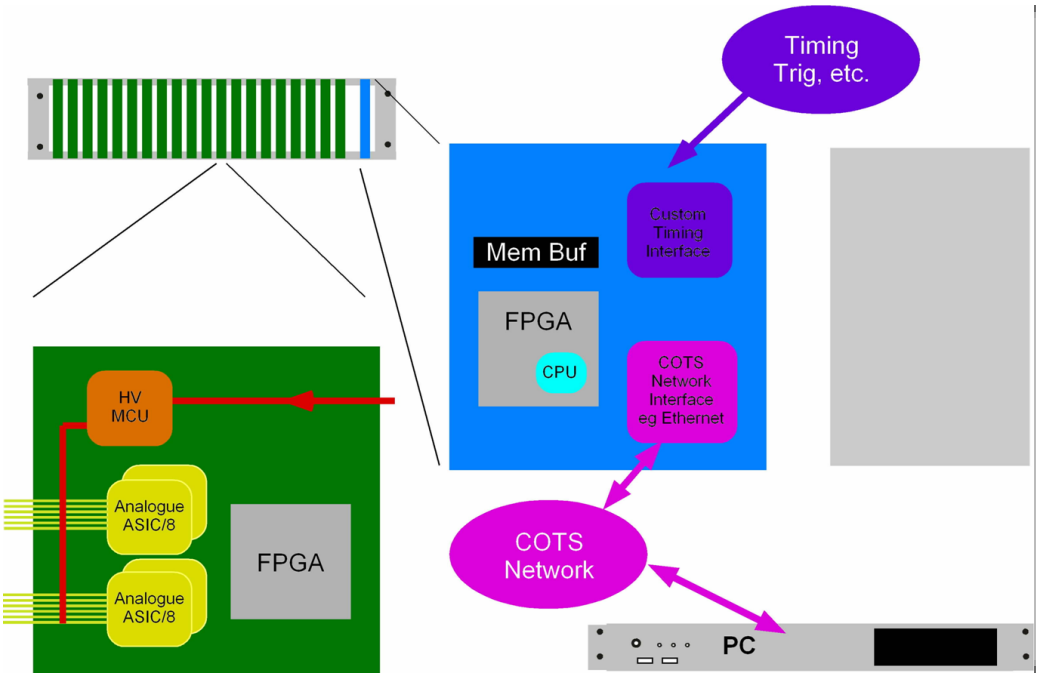


*Fig 5.2 : An overview of the SuperNEMO tracker readout*

An overview of the tracker readout is shown schematically in Fig. 5.2. The component parts are discussed below.

### 5.3.1 Readout Boards

Each readout board handles a number of channels independently. There is no requirement to combine the readout of any specific number of cells, so the number handled by each card will be chosen to allow a convenient size for the boards. If the organization of cables at the detector feedthrough favours a specific grouping, this can be reflected in the design of the cards.

The capture of the analogue signals from the cells is performed by an ASIC, described below. One or more FPGAs will receive data from the ASICs, buffer it and transmit it to the interface board over a high speed serial link. Clock and control signals from the backplane will be supplied to the ASIC and FPGA as appropriate.

Each card will receive a single HV supply from the backplane or from a front panel connection and will fan this out to the cell anodes via steering circuitry that allows the voltage to be ‘tuned’ by up to ~100v or so channel by channel. This allows the operation of each cell to be optimised according

to is Geiger plateau. The ASIC and FPGA can contribute to this steering circuitry, but it is also likely that one or more low cost microcontrollers will be required.

Cost per channel is a major issue for the readout, and this will impact mainly on the readout card. One area of concern is connector costs. The amplifier boards we developed for the 90 cell prototype used captive cables, soldered to the PCBs, but although this offers the lowest cost it is impractical at the channel count of a real module, and for long term operation of the detector. Single pole connectors are too expensive and require too much space; multi-pole connectors are not so commonplace. We will investigate the commercial options but we do not rule out developing a custom connector based on commercial pins in a custom insulator.

### 5.3.2 ASICs

The analogue parts of the readout board will need to be handled by an ASIC to reduce cost and to achieve reasonable channel density. To reduce the development time, the readout board includes one or more FPGAs to handle the 'back end' functionality. In principle, and in the longer term, it would be possible to incorporate this into the ASIC design, but even if there was a cost benefit the flexibility of a freely programmable back end is likely to outweigh that.

The ASIC has to:

- Amplify the input signals from the cell
- Maintain the least significant bits of the timing counters
- Detect and timestamp significant activity the cell
- Transmit hit data synchronously to the back end FPGA
- Receive and decode commands to set threshold etc.
- Provide the analogue functionality required by the HV steering.

To detect pulses on the cathodes a simple amplifier & discriminator is adequate. Hits could be buffered as for the anode signals (below), or could be passed directly to the FPGA – this is a trade off between buffering complexity and pin count on the ASIC.

We need more complicated processing for the anode pulses because we want to use them to cross check or recover longitudinal times. This means extracting three times, the initial leading edge of the pulse, and then the times when the current is reduced sharply, which correspond with the Geiger propagation reaching an end of the cell. Multiple thresholds are of very limited use. Ultimately FADC recording of the pulse is useful, but would consume ASIC resources and increase data size. Preliminary studies have shown good discrimination using peaks in the differential of the signal.

It may be practical to output anode hit 'tokens' directly to the FPGA (e.g. two bits to encode the state of the signal). However, because the cells have a recovery time after each hit it is also practical to multiplex the hit data over a single link. This could be done directly from an alternating pair of buffers, one writing a second readout, or these buffers could be zero suppressed on the chip and copied into a second stage FIFO buffer before readout. This will depend on ASIC channel count, pin constraints, and recovery times as observed from the 90-cell prototype.

The cell-to-cell HV steering might require some analogue service functions from the ASIC; DAC levels, comparators, ADC measurements etc. No part of the ASIC will ever be exposed to HV. These are independent from the readout but are low noise and can safely be included in the same part for reduced costs.

The ASIC will be implemented in a mixed signal technology, for example CX06 0.6 micron from

X-FAB. It is likely we would want to implement 4 or 8 channels in each part, the estimated die size is ~10-20 $mm^2$, and we expect at least 600 good parts per wafer. A prototyping Multi Project Wafer (MPW) run and a Multi Layer Mask (MLM) prototyping run are two options here.
The ASIC design and production will be sub-contracted to the Microelectronics Group at RAL or a specialist commercial contractor.

The funding for the Demonstrator envisages only 1/3 of the ASIC-based detector readout. We are therefore considering replacing ASICs with FPGA-based TDC cards. This option can provide a full readout of all 2000 tracker channels and give an extra flexibility in the readout of the Demonstrator to allow a final tuning of the readout design to be made. This design will use the same front-end and interface boards and crates.

### 5.3.3 Interface Boards

The interface boards collect data from the readout boards (push architecture from the readout boards), buffer it, perform any required additional formatting, and transmit this data to the computing system over Ethernet. The board will probably be based on a FPGA with an embedded processor. It will also receive the clock and control signals, and generate the required clocks, strobes etc. which it distributes to the readout boards over the backplane. We will also include a local interface (USB or similar) for diagnostic or stand alone use, debugging etc

Each crate needs at least one HV supply. This could be from a stand-alone commercial unit, but another option is to use a commercial module built onto the interface board (which will have plenty of free space). We will prototype a standalone HV system based on commercially sourced modules and if successful incorporate this design into the interface card.

To expedite commissioning of the boards we would plan to start firmware development ahead of hardware delivery using a commercial FPGA development board. Prototype interface boards could also be tested (out of crate) using commercial FPGA development boards emulating the readout boards.

### 5.3.4 Custom Crates

The tracking readout sub-module is based on a custom crate housed in standard 19inch racks. It will be constructed from ‘off the shelf’ (eurocard) mechanics and power supplies coupled to a custom backplane. The form factor will be determined by the size required for the readout cards (ie the number of channels handled by each card). Provision for spare slots will be built in to allow for damage/failures etc.

### 5.3.5 DAQ & Timing Infrastructure

The readout system is based around sub-modules that are connected using commercial Ethernet. Each sub-module provides ample buffering so that the performance of the networks (latency etc.) is not critical. We expect to broadcast the data to a number of primary computing nodes each of which records a full set of data, and which could then distribute data to ‘worker’ nodes as required. The worker nodes could, for example, be located at remote labs.

The timing system is used to generate a global clock and to synchronise all parts of the system using a serial command stream distributed together with the clock to each sub-modules. These commands would be global, but could be used to synchronise commands previously loaded via the network. The timing system would also incorporate a real time clock with an accurate external reference (eg, GPS, MSF-60, DCF-77 etc.) so that the local reference timing can be converted to real times.

### 5.3.6 Testing during Cell Production

The existing NEMO-III based TDC system and FADC systems used on the 90-cell prototype will be available for production testing of the cells at Manchester and integration at MSSL. The existing equipment is adequate to cover these needs.

## 5.4 Calorimeter readout

The calorimeter readout electronics is being developed by the Caen group.

# 6.0 Double beta decay source

A key design feature of SuperNEMO is the ability to measure different isotopes since the source is separated from the detector. The choice of the isotope is affected by several parameters. These include the transition energy ($Q_{\beta\beta}$), the nuclear matrix elements, the background in the energy region of interest, the half-life of the standard model allowed $2\nu\beta\beta$ decay, purification feasibility, isotopic abundance of the candidate and the feasibility of enrichment. The baseline isotope choice for SuperNEMO is Se82.

The enrichment of Se82 (and most likely other isotopes to be used in SuperNEMO) will be carried out in Russia using a centrifugation method. The technology of the source foil production (with a thickness of 40-60 mg/cm$^2$) is being developed by LAL (Orsay), ITEP (Moscow) and INL (USA).

This Chapter is under construction.

# 7.0 Detector radiopurity

To reach the target sensitivity the SuperNEMO detector materials will have to be extremely radio-pure. The most dangerous sources of radioactive backgrounds are Bi214 and Tl208 from the U238 and Th232 chains respectively located in the source foil or coming from Rn in the tracker. Three main methods are used to measure these very low levels of radioactive contamination: $\gamma$-spectrometry with HPGe detectors, Bi-Po delayed coincidence measurement with a dedicated BiPo detector (for the source foil survey) and Rn emanation measurements from the detector materials.

## 7.1 $\gamma$-spectroscopy with HPGe detectors

All detector materials will be screened by low background HPGe detectors. Pre-screening will be used for initial selection of the materials with a sensitivity to Bi214 and Tl208 at a few mBq/kg level. The materials inside the fiducial volume of the detector will undergo further measurements. 400/600 cm$^3$ detectors at LSM can reach sensitivities of 0.2 mBq/kg and 0.06 mBq/kg to Bi214 and Tl208 respectively with a 1kg sample after 1 month of measurements.

This section is under construction.

## 7.2. BiPo detector

The acceptable levels of the radioactive contamination in the SuperNEMO source foils are too low to be measured with HPGe detectors. In addition the geometry of a thin, large area foil is not suitable for HPGe measurements. In order to measure the radiopurity of the source foils at the level of 2 and 10 μBq/kg for Tl208 and Bi214 respectively a special BiPo detector has been developed.

A BiPo-1 detector which has been running in LSM has demonstrated the feasibility of the required sensitivity. A BiPo-3 detector is being constructed and will be used to measure the Se82 source foil for the Demonstrator module.

This section is under construction.

## 7.3 Rn measurements in the tracker.

Rn is one of the most serious sources of background in the experiments searching for ultra-rare processes. For SuperNEMO Rn222, together with Bi214 and Tl208 contaminations inside the source foil, is the main source of the background. Rn222 is a daughter of the U-Ra chain with a half-life of 3.8 days. It can mimic ββ events when its daughter, Bi214, is deposited on the source foil or tracker cathode wires close to the foil. In addition, Rn220 from the Th232 chain, the so-called thoron, leading to Tl208 can also be a dangerous source of the background although due to a short half-life of 52 sec, it has much less time to diffuse inside the detector compared to Rn222.

Rn can penetrate the detector from the outside lab relatively easily. SuperNEMO will use an anti-radon factory similar to the one used for NEMO-III to reduce the amount of Rn in the vicinity of the detector [10]. Special attention will be paid to the gas tightness of the detector joints. Apart from external Rn there are also internal sources: the emanation of Rn from the detector material.

To reach the target sensitivity of $10^{26}$ yr the required level of Rn concentration inside the tracking chamber is $\leq$ 0.15 mBq/m$^3$. For comparison, the Rn concentration in NEMO-III is 5 mBq/m$^3$. HPGe γ-spectroscopy and Rn emanation measurements will be used to select materials to reach these low concentrations. However the Rn concentration inside the detector also depends on the integration processes. Because of that, and also due to low activities involved, Rn levels in the tracker will have to be monitored in parallel with the detector construction and integration. The Rn content will be analysed in the tracker sub-modules as they are built.

Detecting Rn concentration at such low levels is challenging. Commercial Rn detectors have sensitivities at the order of few 100 mBq/m$^3$ at best. A purpose built Rn detector currently employed in LSM has a sensitivity of 1 mBq/m$^3$.

To reach the sensitivity of ~0.1 mBq/m$^3$ a Rn concentration technique will be used. A schematic design of a Rn concentration line to be used is shown in Fig. 7.1

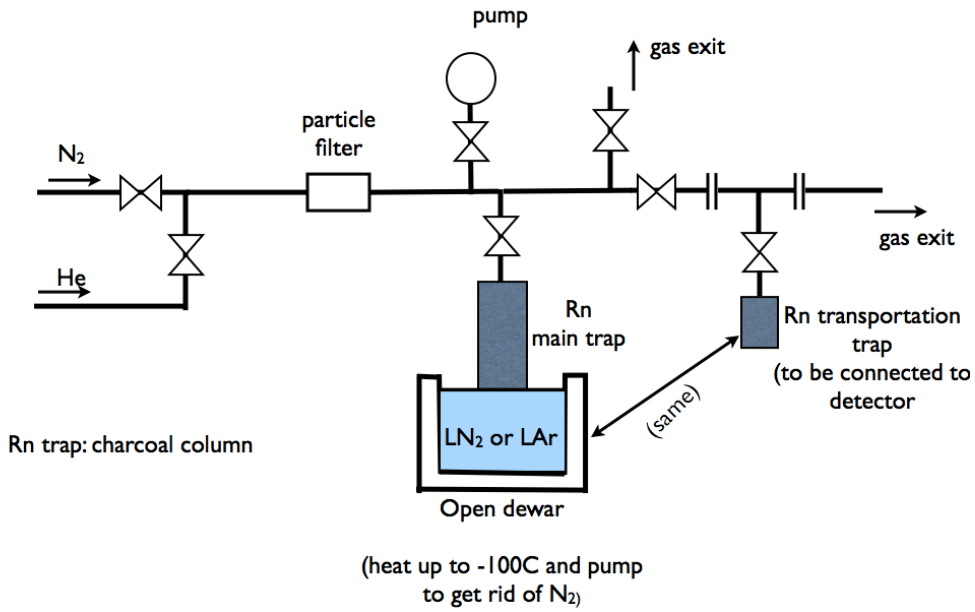


*Fig. 7.1 Rn concentration line to be used for Rn measurements in the tracker sub-modules.*

The key element of the line is a charcoal absorber based on an ultra-pure activated carbon product. The charcoal column is cooled to liquid nitrogen temperatures and the gas from a cylinder or a tracker sub-module (or from an emanation chamber) is passed through the line. Rn is concentrated inside the trap which is then evacuated at -100C to get rid of $N_2$ and subsequently heated to move the Rn atoms to a small transportation trap. Rn is then transferred into an electrostatic detector shown in Fig. 7.2

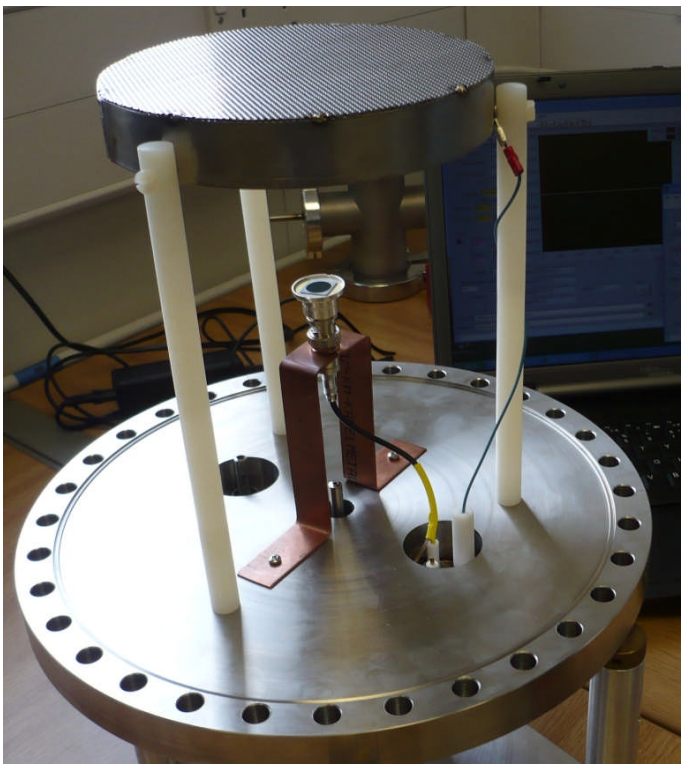

*Fig 7.2 Electrostatic Rn detector with a drift electrode at the top and windowless PIN photodiode in the centre.*

The detector is a cylindrical vessel with a positively charge electrode which acts as an electrostatic concentrator for positively charged daughters of the Rn222 decay. The Rn daughters are attracted to a windowless PIN photodiode which detects α particles. The decays of Po218, Po214 and Po210 are distinguished by mono-energetic peaks in the energy spectrum. A Hamamatsu S3204-09 PIN photodiode will be used with a surface area of 18mm x 18mm and a thickness of 0.3 mm operated at a reverse bias voltage of -10-30V. The PIN photodiode will be coupled to a low noise pre-amplifier.

The sensitivity of the method is given by

$$R \leq N_{90\%CL} / (V\tau\, \varepsilon(1-e^{-t/\tau})$$

where $N$ is an upper bound on the number of counts at 90%CL, $V$ is the volume from which Rn is concentrated ($V$ = 4m$^3$ for the tracker 1C sub-module), $\tau$ is the life-time of Rn222, $\varepsilon$ is a combined detector and Rn transfer efficiency and $t$ is the measurement time. With a detection efficiency of 10%, 5 days of data taking and 4m$^3$ of the assayed volume the sensitivity is at the required level of 0.1 mBq/m$^3$. Preliminary estimates have shown that lower backgrounds and higher efficiencies should be feasible.

The Rn concentration line and the detector will first be used to measure a large variety of pure commercial gases to identify the manufacturer with the required radiopurity for Rn. It will then be used for measuring Rn in tracker sub-modules as they are built. The line and detector will also be used for Rn emanation measurements of the detector materials.

# 8.0 Passive shielding

Passive shielding protects the detector from external gamma rays and neutrons. SuperNEMO will use water passive shielding. The possibility to use instrumented (with PMTs) ultra-pure water or liquid scintillator to tag high energy cosmic muons is under consideration.

The Chapter is under construction.

# 9.0 Installation and commissioning at LSM

After October 2012, the Demonstrator modules will be moved to the Modane Underground Laboratory (LSM). The detector will be taken apart into its transportable sub-modules and reassembled in clean surface laboratory at LSM. Initial assembly and detailed integration checks will take place here due to major space and working constraints underground. Only top and bottom veto calorimeter blocks will be installed at the Nu-Lab. Consequently the integration of the main calorimeter part, the calorimeter walls, will be done at LSM.
The precise integration process is to be finalised but it is expected that most of the assembly procedures will take place at the ground level laboratory. The calorimeter mechanical design and overall integration is a responsibility of the French collaborators with a very active participation of the UK personnel in particular in the tracker integration task.

The exact location of the Demonstrator will depend on the status of the LSM extension project ULISSE. However, if the new cavern is not available on Demonstrator time scale, the detector will be installed in place of the decommissioned NEMO-III detector. This has been agreed with the LSM and IN2P3 management. The design and especially dimensions of the Demonstrator have to therefore take into account the constraints of the current LSM underground laboratory.

This Chapter is under construction.

# 10.0 Management (UK only)

## 10.1 Organisation (UK only)

A similar organisation and management structure will be used, as in the design study; with the individual work packages being lead by Technical Managers (see Fig 10.1). Decisions will be made by the Technical Board, Executive Board and/or ultimately the UK Spokesperson, with support from the Project Manager (see Fig. 10.2)

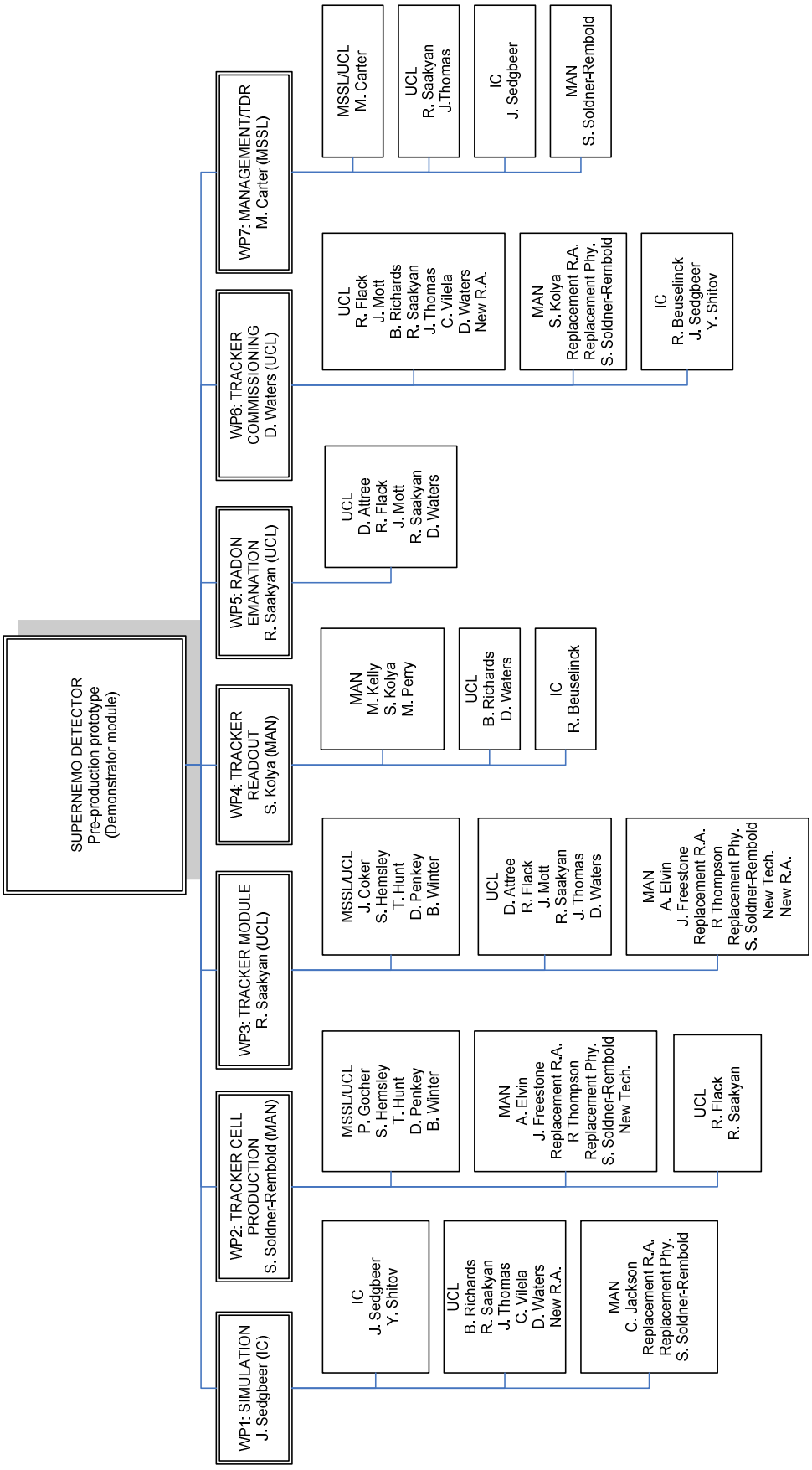


*Fig 10.1 : Team Organisation by Work Package*

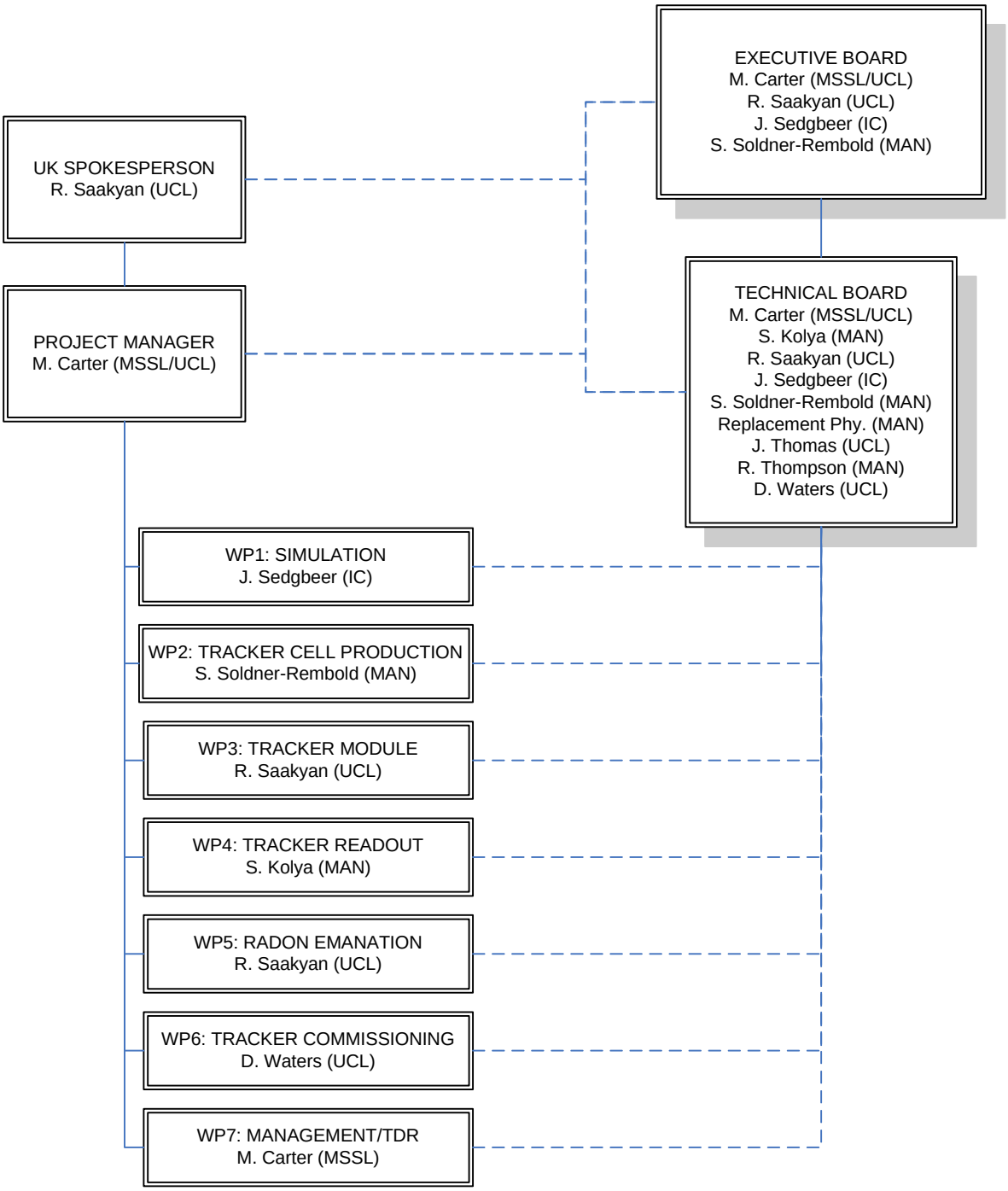


*Fig 10.2 : Management Organisation*

The Technical Managers will each lead a team of scientists, engineers and technicians and are responsible for ensuring that the tasks in their specific work package are completed in line with the project schedule. They will report directly to the Project Manager on matters of technical progress & other issues and on the management of the day-to-day activities of their team.

The Technical Board will be responsible for ensuring that the overall project requirements are met and for making technical recommendations to the Executive Board. The various members of the Technical Board will also form the review panels needed at critical stages/milestones of the project.

The Executive Board is to be made up of the Institute Managers from each of the University groups. They will be responsible for approving any key/major technical decisions, deploying and monitoring their group resources and reporting on their group expenditure to the Project Manager.

Ultimately, all major decisions and any important project issues will have to be resolved and/or sanctioned by the UK Spokesperson (R. Saakyan, UCL). He will have overall authority for all UK SuperNEMO matters and works closely with the Project Manager to ensure that the project is successful, on time and within budget. Any decisions e.g. de-scoping the project or re-directing resources to other/new tasks/goals must be made by the UK spokesperson and agreed by the Project Manager and Executive Board.

In this construction phase of the pre-production prototype (Demonstrator module), it is expected that more detailed planning of activities and tracking of parts will be required. This is due to the large quantities involved and the need for two production sites. Also, it will be essential to ensure that all members of the team work closely together with regular telecons/meetings and periodic reviews to ensure that production progresses smoothly. In addition, appropriate documentation will be needed to log procedures, construction details and track parts.

## 10.2 Milestones and Schedule (UK only)

The milestones can be found in appendix A and the schedule, associated with these milestones, can be found in appendix B.

## 10.3 Costs (UK only)

The three SuperNEMO research grants that have been awarded by STFC are shown in appendix C, along with additional breakdowns of some of the costs. It is understood that the FTEs for the three rolling grants (also in appendix C) have been agreed. However, the costs associated with these FTEs are not yet available as these grants are still being assessed by the university groups.

## 10.4 Risk Register (UK only)

The risk register includes the effects of the risks on schedule and contingency. There are now three additional columns containing the mitigation costs, schedule impact and “cost x probability” estimates. These additional columns showed that a contingency level of 10% is appropriate for this project. See appendix D.

# Appendix A: Milestones (UK only)

(red font = review point)

| Milestone no. | Work package | Milestone | Completion Date |
|---|---|---|---|
| M1.1 | WP1: Simulation | Simulation of final demonstrator module design implemented | 26 Jul 2010 |
| M1.2 | WP1: Simulation | Standardise Grid usage for software | 26 Jul 2010 |
| **M1.3** | **WP1: Simulation** | **Software & simulation portion of TDR complete** | **26 May 2011** |
| M1.4 | WP1: Simulation | Demonstrator module data analysis software complete | 28 Nov 2011 |
| **M1.5** | **WP1: Simulation** | **Demonstrator commissioning results: software performance v simulation** | **01 Jun 2012** |
| M1.6 | WP1: Simulation | Preliminary results available | 31 Oct 2012 |
| M2.1 | WP2: Tracker Cell Production | Test system design/specification complete | 06 Sep 2010 |
| M2.2 | WP2: Tracker Cell Production | Cell components & cables sourced. | 23 Aug 2010 |
| M2.3 | WP2: Tracker Cell Production | First individual robot mechanisms operational | 04 Aug 2010 |
| **M2.4** | **WP2: Tracker Cell Production** | **Final robot sequencing complete** | **28 Feb 2011** |
| **M2.5** | **WP2: Tracker Cell Production** | **Cell test system demonstrated** | **16 Feb 2011** |
| M2.6 | WP2: Tracker Cell Production | Clean component handling systems demonstrated | 14 Feb 2011 |
| **M2.7** | **WP2: Tracker Cell Production** | **Production readiness review** | **11 Apr 2011** |
| M2.8 | WP2: Tracker Cell Production | Start cell production | 02 May 2011 |
| **M2.9** | **WP2: Tracker Cell Production** | **Complete cell production** | **07 Dec 2011** |

| Milestone no. | Work package | Milestone | Completion Date |
|---|---|---|---|
| M3.1 | WP3: Tracker Module | Bars versus block design decision (calorimeter) | 08 Feb 2010 |
| M3.2 | WP3: Tracker Module | Test set up definition | 08 Feb 2010 |
| M3.3 | WP3: Tracker Module | Gamma tag removal | 08 Feb 2010 |
| M3.4 | WP3: Tracker Module | Working Tracker Module | 15 Feb 2012 |
| M4.1 | WP4: Tracker Readout | HV steering design complete | 26 Jul 2010 |
| M4.2 | WP4: Tracker Readout | Detector connection and infrastructure specifications complete | 26 Jul 2010 |
| M4.3 | WP4: Tracker Readout | ASIC specification | 02 Sep 2010 |
| M4.4 | WP4: Tracker Readout | Design of readout boards, interface cards & custom crate complete | 17 Jan 2011 |
| **M4.5** | **WP4: Tracker Readout** | **Working DAQ only (without ASICs or HV)** | **20 Jun 2011** |
| M4.6 | WP4: Tracker Readout | Delivery of ASICs | 15 Aug 2011 |
| M4.7 | WP4: Tracker Readout | Working prototype readout | 18 Oct 2011 |
| **M4.8** | **WP4: Tracker Readout** | **Full readout complete** | **03 Feb 2012** |
| M4.9 | WP4: Tracker Readout | Delivery of readout to MSSL | 20 Feb 2012 |
| **M4.10** | **WP4: Tracker Readout** | **Readout integrated with Tracker Module** | **15 Jun 2012** |
| M5.1 | WP5: Radon Emanation | Final radon detector choice | 03 Oct 2011 |
| M7.1 | WP7: Management | Define documentation system, meeting requirements etc. | 04 May 2010 |

| Milestone no. | Work package | Milestone | Completion Date |
|---|---|---|---|
| M7.2 | WP7: Management | Review financial reporting system with Institute Managers | 04 May 2010 |
| M7.3 | WP7: Management | Review production process (tracking items, reporting system etc) | 17 Nov 2010 |
| M7.4 | WP7: Management | Organise production readiness reviews | 25 Feb 2011 |
| M7.5 | WP7: Management | Provisional version of full TDR | 25 Jul 2011 |
| M7.6 | WP7: Management | Full TDR complete | 23 Jan 2012 |
| M7.7 | WP7: Management | Submission of a SuperNEMO full construction proposal | 07 May 2012 |

# Appendix B: Schedule (UK only)

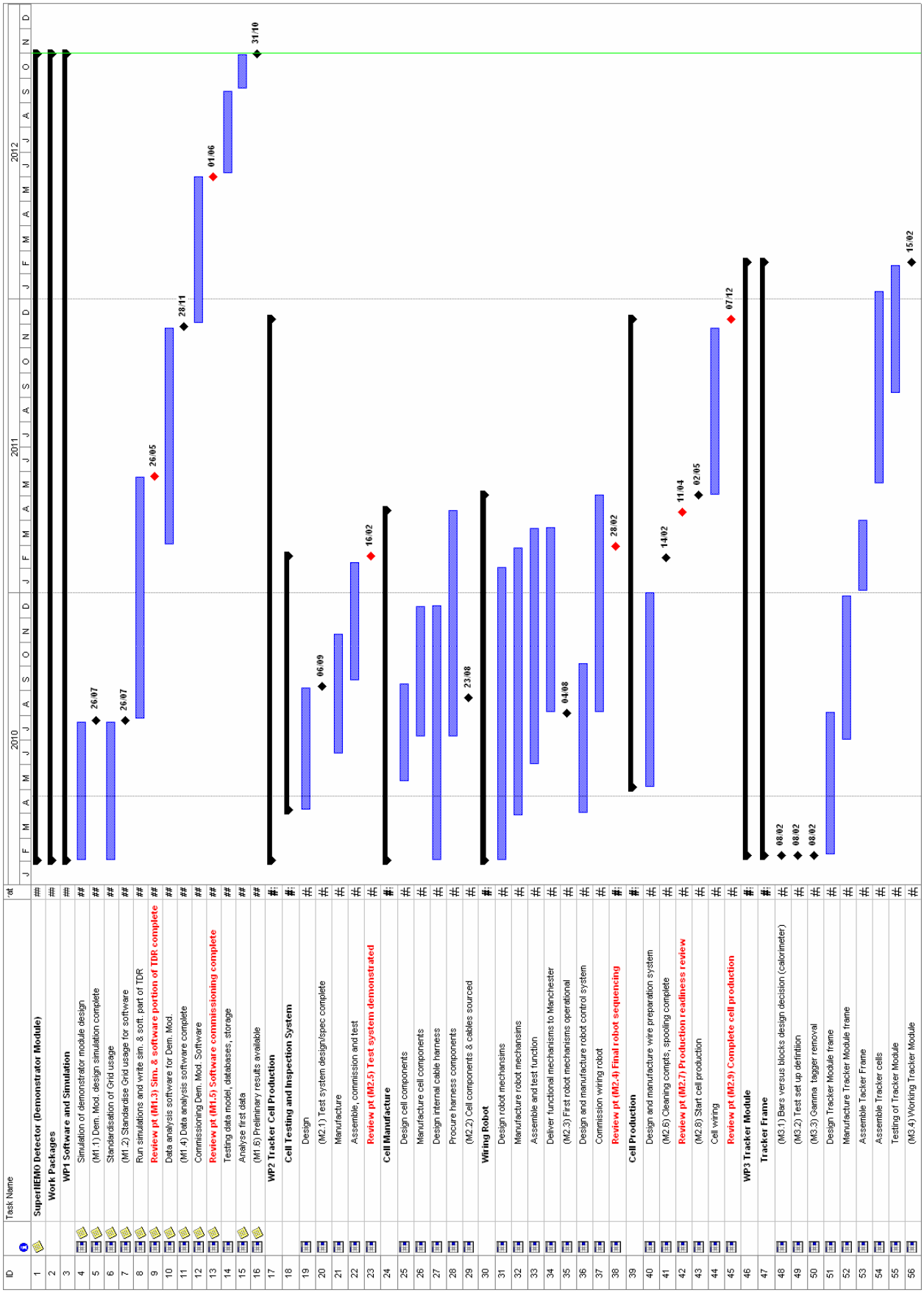

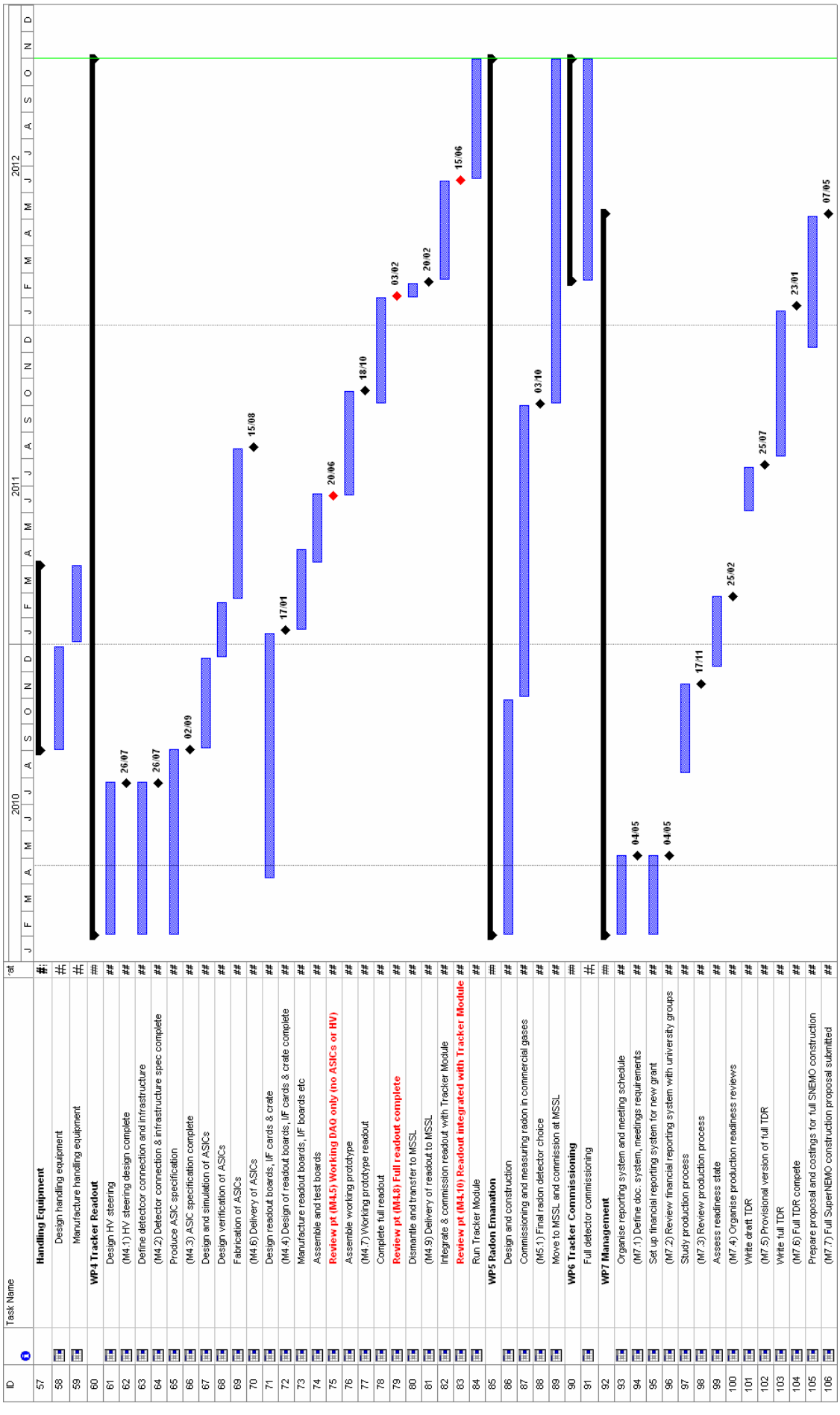
ID
Task Name
Handling Equipment
Design handling equipment
Manufacture handling equipment
WP4 Tracker Readout
Design HV steering
(M4.1) HV steering design complete
Define detector connection and infrastructure
(M4.2) Detector connection & infrastructure spec complete
Produce ASIC specification
(M4.3) ASIC specification complete
Design and simulation of ASICs
Design verification of ASICs
Fabrication of ASICs
(M4.6) Delivery of ASICs
Design readout boards, IF cards & crate
(M4.4) Design of readout boards, IF cards & crate complete
Manufacture readout boards, IF boards etc
Assemble and test boards
Review pt (M4.5) Working DAQ only (no ASICs or HV)
Assemble working prototype
(M4.7) Working prototype readout
Complete full readout
Review pt (M4.8) Full readout complete
Dismantle and transfer to MSSL
(M4.9) Delivery of readout to MSSL
Integrate & commission readout with Tracker Module
Review pt (M4.10) Readout integrated with Tracker Module
Run Tracker Module
WP5 Radon Emanation
Design and construction
Commissioning and measuring radon in commercial gases
(M5.1) Final radon detector choice
Move to MSSL and commission at MSSL
WP6 Tracker Commissioning
Full detector commissioning
WP7 Management
Organise reporting system and meeting schedule
(M7.1) Define doc. system, meetings requirements
Set up financial reporting system for new grant
(M7.2) Review financial reporting system with university groups
Study production process
(M7.3) Review production process
Assess readiness state
(M7.4) Organise production readiness reviews
Write draft TDR
(M7.5) Provisional version of full TDR
Write full TDR
(M7.6) Full TDR compete
Prepare proposal and costings for full SNEMO construction
(M7.7) Full SuperNEMO construction proposal submitted
2010
2011
2012
26/07
26/07
02/09
17/01
15/08
20/06
18/10
03/02
20/02
15/06
04/05
04/05
17/11
25/02
03/10
25/07
23/01
07/05

# Appendix C: Costs (UK only)

## C.1 SuperNEMO: Total Project Grant only

**FUNDING DETAILS:**

| Summary Fund Heading | Fund Heading | Full Economic Costs £ | Research Council contribution % | Research Council contribution £ |
|---|---|---|---|---|
| **Directly Incurred** | | | | |
| | Other staff | £796,926.00 | 80% | £637,540.77 |
| | Equipment | £100,000.04 | 80% | £79,999.96 |
| | Other DI costs | £190,609.25 | 80% | £152,487.38 |
| | Travel & subsistence | £127,595.64 | 80% | £102,076.55 |
| | **Sub-total** | **£1,215,130.92** | **80%** | **£972,104.67** |
| **Directly Allocated** | | | | |
| | Estates Costs | £138,430.04 | 80% | £110,744.00 |
| | Other DA staff | £101,076.90 | 80% | £80,861.52 |
| | Other DA costs | £126,651.25 | 80% | £101,321.00 |
| | Investigator DA | £138,616.65 | 80% | £110,893.32 |
| | **Sub-total** | **£504,774.84** | **80%** | **£403,819.84** |
| **Indirect Costs** | | | | |
| | Indirect Costs FeC | £395,310.85 | 80% | £316,248.68 |
| | **Sub-total** | **£395,310.85** | **80%** | **£316,248.68** |
| **Exceptions** | | | | |
| | Equipment | £717,999.96 | 100% | £717,999.96 |
| | **Sub-total** | **£717,999.96** | **100%** | **£717,999.96** |
| | **Total** | **£2,833,216.56** | **85%** | **£2,410,173.15** |

**GRANT PERIOD: 36 months** **STARTS: 01/11/2009** **ENDS: 31/10/2012**

# C.2 University College London: Project Grant only (expected re-announcement)

**STFC Ref: ST/H000607/1**

**PROJECT TITLE: SuperNEMO Demonstrator Module Construction**

**PRINCIPAL INVESTIGATOR (OR RESEARCH FELLOW): Dr R Saakyan**

**INSTITUTION: University College London**

**FUNDING DETAILS:**

| Summary Fund Heading | Fund Heading | Full Economic Costs £ | Research Council contribution % | Research Council contribution £ |
|---|---|---|---|---|
| **Directly Incurred** | | | | |
| | Other staff | £459,541.93 | 80% | £367,633.54 |
| | Equipment | £50,000.00 | 80% | £40,000.00 |
| | Other DI costs | £175,268.93 | 80% | £140,215.14 |
| | Travel & subsistence | £57,434.14 | 80% | £45,947.31 |
| | **Sub-total** | **£742,245.00** | **80%** | **£593,796.00** |
| **Directly Allocated** | | | | |
| | Estates Costs | £54,682.10 | 80% | £43,745.68 |
| | Other DA staff | £101,076.90 | 80% | £80,861.52 |
| | Other DA costs | £126,651.25 | 80% | £101,321.00 |
| | Investigator DA | £138,616.65 | 80% | £110,893.32 |
| | **Sub-total** | **£421,026.90** | **80%** | **£336,821.52** |
| **Indirect Costs** | | | | |
| | Indirect Costs FeC | £161,419.03 | 80% | £129,135.22 |
| | **Sub-total** | **£161,419.03** | **80%** | **£129,135.22** |
| **Exceptions** | | | | |
| | Equipment | £150,000.00 | 100% | £150,000.00 |
| | **Sub-total** | **£150,000.00** | **100%** | **£150,000.00** |
| | **Total** | **£1,474,690.92** | **82%** | **£1,209,752.74** |

**GRANT PERIOD: 36 months** **STARTS: 01/11/2009** **ENDS: 31/10/2012**

**STAFF DETAILS**

| Fund Heading | Name | Months on Project | %FTE per year | Start date |
|---|---|---|---|---|
| DI staff | R. Flack | 36 | 50% | 01/11/2009 |
| | M. Carter | 36 | 60% | 01/11/2009 |
| | T. Hunt | 36 | 100% | 01/11/2009 |
| | J. Coker | 36 | 43% | 01/11/2009 |
| | S. Hemsley | 36 | 66% | 01/11/2009 |
| | D. Penkey | 36 | 53% | 01/11/2009 |
| DA staff | R. Saakyan | 36 | 60% | 01/11/2009 |
| | B. Winter | 36 | 10% | 01/11/2009 |
| | B. Anderson | 12 | 80% | 01/11/2009 |

**EQUIPMENT DETAILS**

| Work Package | Description | fEC |
|---|---|---|
| WP2: Cell Production | Clamp pin feeder | £10,000 |
| | Pick & place tools | £15,000 |
| | Clamp/cut for 1st cell | £5,000 |
| | Actuator | £15,000 |
| | Elec positioning system | £15,000 |
| | Elec. Wire feed & tension | £15,000 |
| | Robot table | £5,000 |
| | *Sub-total* | *£80,000* |
| WP3: Tracker frame | Tracker frame | £50,000 |
| | Cells, clamp pins, copper | £40,000 |
| | Handling equipment | £30,000 |
| | *Sub-total* | *£120,000* |
| | **Total** | **£200,000** |

**OTHER DI COSTS**

| Work Package | Description | fEC |
|---|---|---|
| WP2: Cell Production | Sub contract P. Gocher | £95,054 |
| | *Sub-total* | *£95,054* |
| WP3: Tracker frame & radon emanation | Physics -MAPS w/shop | £18,400 |
| | Recruitment/adverts | £500 |
| | Other (Radon and gas) | £50,000 |
| | *Sub-total* | *£68,900* |
| | **Total** | **£163,954** |

# C.3 The University of Manchester: Project Grant only

**STFC Ref: ST/H000615/1**

**PROJECT TITLE: SuperNEMO Demonstrator Module Construction**

**PRINCIPAL INVESTIGATOR (OR RESEARCH FELLOW): Dr S Soldner-Rembold**

**INSTITUTION: The University of Manchester**

**FUNDING DETAILS:**

| Summary Fund Heading | Fund Heading | Full Economic Costs £ | Research Council contribution % | Research Council contribution £ |
|---|---|---|---|---|
| **Directly Incurred** | | | | |
| | Other staff | £204,911.28 | 80% | £163,929.01 |
| | Equipment | £50,000.04 | 80% | £39,999.96 |
| | Other DI costs | £15,340.32 | 80% | £12,272.24 |
| | Travel & subsistence | £56,738.70 | 80% | £45,391.02 |
| | **Sub-total** | **£326,990.34** | **80%** | **£261,592.23** |
| **Directly Allocated** | | | | |
| | Estates Costs | £37,343.46 | 80% | £29,874.76 |
| | Other DA staff | £0.00 | 80% | £0.00 |
| | Other DA costs | £0.00 | 80% | £0.00 |
| | Investigator DA | £0.00 | 80% | £0.00 |
| | **Sub-total** | **£37,343.46** | **80%** | **£29,874.76** |
| **Indirect Costs** | | | | |
| | Indirect Costs FeC | £100,676.50 | 80% | £80,541.20 |
| | **Sub-total** | **£100,676.50** | **80%** | **£80,541.20** |
| **Exceptions** | | | | |
| | Equipment | £567,999.96 | 100% | £567,999.96 |
| | **Sub-total** | **£567,999.96** | **100%** | **£567,999.96** |
| | **Total** | **£1,033,010.25** | **91%** | **£940,008.15** |

**GRANT PERIOD: 36 months** **STARTS: 01/11/2009** **ENDS: 31/10/2012**

**STAFF DETAILS**

| Fund Heading | Name | Months on Project | %FTE per year | Start date |
|---|---|---|---|---|
| DI staff | RA - Irina Nasteva | 35 | 92% | 01/11/2009 |
| | New Technician | 36 | 67% | 01/11/2009 |

**EQUIPMENT DETAILS**

| Work Package | Description | | fEC |
|---|---|---|---|
| WP2: Cell Production | Trakus wire | | £12,000 |
| | Wire spooling cleaning station | | £15,000 |
| | Copper cleaning station | | £5,000 |
| | Purged storage | | £5,000 |
| | Database PC and bar code components | | £2,000 |
| | Laminar air shower above wiring robot | | £15,000 |
| | Wire tension mesurement | | £5,000 |
| | Optical inspection of wired cell and endcaps | | £15,000 |
| | Control system for robot (des, int and test) | | £11,000 |
| | Vacuum system | | £10,000 |
| | Test tank, gas handling, elecs, trigger | | £40,000 |
| | Cell storage cassettes & cabling | | £30,000 |
| | Transfer system to move wired cells | | £30,000 |
| | Storage rack and handling tested cassettes | | £5,000 |
| | Transport container for shipping cassettes to MSSL | | £5,000 |
| | Shipping costs (Manchester to MSSL return) | | £5,000 |
| | Clean room tent (Manchester) | | £10,000 |
| | Cabling and feedthroughs | | £60,000 |
| | | *Sub-total* | *£280,000* |
| WP4: Tracker Readout | ASICS: | MPW run | £20,000 |
| | | Custom fab run | £30,000 |
| | | Packaging (for this module only) | £20,000 |
| | Readout boards: | FPGA development (4+) | £5,000 |
| | | Custom connector development | £10,000 |
| | | Prototype run (2 boards) | £10,000 |
| | | Production run (150 boards) | £15,000 |
| | | Test stand & fixtures | £5,000 |
| | Custom crate: | Std metal work for 10 crates | £8,000 |
| | | PSUs | £8,000 |
| | | Proto backplane (2) | £4,000 |
| | | Production backplane (10) | £8,000 |
| | Interface Boards: | FPGA development board | £2,000 |
| | | IP cores/licences | £2,000 |
| | | Prototype run (2 boards) | £8,000 |
| | | Production run (10 boards) | £18,000 |
| | | HV (modules & prototyping) | £10,000 |
| | DAQ Infrastructure: | | £15,000 |
| | ASIC engineering: | | £140,000 |
| | | *Sub-total* | *£338,000* |
| | | **Total** | **£618,000** |

# C.4 Imperial College London: Project Grant only

**STFC Ref: ST/H000577/1**

**PROJECT TITLE: SuperNEMO Demonstrator Module Construction**

**PRINCIPAL INVESTIGATOR (OR RESEARCH FELLOW): Dr J Sedgbeer**

**INSTITUTION: Imperial College London**

**FUNDING DETAILS:**

| Summary Fund Heading | Fund Heading | Full Economic Costs £ | Research Council contribution % | Research Council contribution £ |
|---|---|---|---|---|
| **Directly Incurred** | | | | |
| | Other staff | £132,472.79 | 80% | £105,978.22 |
| | Equipment | £0.00 | 80% | £0.00 |
| | Other DI costs | £0.00 | 80% | £0.00 |
| | Travel & subsistence | £13,422.80 | 80% | £10,738.22 |
| | **Sub-total** | **£145,895.59** | **80%** | **£116,716.44** |
| **Directly Allocated** | | | | |
| | Estates Costs | £46,404.48 | 80% | £37,123.56 |
| | Other DA staff | £0.00 | 80% | £0.00 |
| | Other DA costs | £0.00 | 80% | £0.00 |
| | Investigator DA | £0.00 | 80% | £0.00 |
| | **Sub-total** | **£46,404.48** | **80%** | **£37,123.56** |
| **Indirect Costs** | | | | |
| | Indirect Costs FeC | £133,215.32 | 80% | £106,572.26 |
| | **Sub-total** | **£133,215.32** | **80%** | **£106,572.26** |
| **Exceptions** | | | | |
| | Equipment | £0.00 | 100% | £0.00 |
| | **Sub-total** | **£0.00** | **100%** | **£0.00** |
| | **Total** | **£325,515.39** | **80%** | **£260,412.26** |

**GRANT PERIOD: 36 months** **STARTS: 01/11/2009** **ENDS: 31/10/2012**

**STAFF DETAILS**

| Fund Heading | Name | Months on Project | %FTE per year | Start date |
|---|---|---|---|---|
| DI staff | Y. Shitov | 36 | 100% | 01/11/2009 |

## C.5 SuperNEMO: Rolling Grant (UK only) - PPGP FTE recommendation

It is understood that the FTEs below have been agreed. However, the costs associated with these FTEs are not yet available as these grants are still being assessed by the university groups.

| Institute | Name | Category | 2009/10 | 2010/11 | 2011/12 | 2012/13 | 2013/14 | 2014/15 |
|---|---|---|---|---|---|---|---|---|
| Imperial N | Sedgbeer, Julia | Ac | 0.10 | 0.20 | 0.20 | 0.20 | 0.20 | 0.10 |
| Imperial N | Shitov, Y. | Ph | 0.00 | 0.00 | 0.00 | 0.75 | 0.50 | 0.00 |
| Imperial N | Beuselinck | PP | 0.17 | 0.30 | 0.40 | 0.40 | 0.40 | 0.20 |
| Imperial N | Barber, G | E | 0.00 | 0.00 | 0.10 | 0.10 | 0.10 | 0.10 |
| Imperial N | Clark, I | T | 0.00 | 0.10 | 0.10 | 0.10 | 0.10 | 0.05 |
| Imperial N | Hare, R | T | 0.00 | 0.10 | 0.10 | 0.10 | 0.10 | 0.05 |
| **Total FTE** | | | **0.27** | **0.70** | **0.90** | **1.65** | **1.40** | **0.50** |
| Manchester | Soeldner-Rembold, S | Ac | 0.00 | 0.00 | 0.07 | 0.10 | 0.10 | 0.06 |
| Manchester | Snow, S | Ph | 0.25 | 0.50 | 0.50 | 0.50 | 0.50 | 0.25 |
| Manchester | Kelly, M | AP | 0.25 | 0.50 | 0.45 | 0.30 | 0.20 | 0.15 |
| Manchester | Kolya, S | AP | 0.25 | 0.50 | 0.55 | 0.40 | 0.30 | 0.15 |
| Manchester | Freestone, J | E | 0.25 | 0.50 | 0.50 | 0.50 | 0.50 | 0.25 |
| Manchester | Thompson, R | E | 0.25 | 0.50 | 0.50 | 0.50 | 0.50 | 0.25 |
| Manchester | Elvin, A | T | 0.25 | 0.00 | 0.00 | 0.00 | 0.00 | 0.00 |
| Manchester | Perry, M | T | 0.25 | 0.00 | 0.00 | 0.00 | 0.00 | 0.00 |
| **Total FTE** | | | **1.75** | **2.50** | **2.57** | **2.30** | **2.10** | **1.11** |
| UCL | Ruben Saakyan | Ac | 0.08 | 0.17 | 0.17 | 0.20 | 0.20 | 0.10 |
| UCL | Jenny Thomas | Ac | 0.02 | 0.05 | 0.11 | 0.13 | 0.15 | 0.07 |
| UCL | David Waters | Ac | 0.04 | 0.08 | 0.15 | 0.15 | 0.15 | 0.07 |
| UCL | Nemo/SuperNemo RA | Ph | 0.00 | 0.00 | 0.25 | 1.00 | 0.50 | 0.00 |
| UCL | Alexey Lyapin | AP | 0.10 | 0.20 | 0.20 | 0.20 | 0.20 | 0.10 |
| UCL | Gianfranco Sciacca | AP | 0.25 | 0.00 | 0.00 | 0.00 | 0.00 | 0.00 |
| UCL | Brian Anderson | E | 0.40 | 0.00 | 0.00 | 0.00 | 0.00 | 0.00 |
| UCL | Derek Attree | T | 0.25 | 0.50 | 0.50 | 0.50 | 0.50 | 0.25 |
| **Total FTE** | | | **1.15** | **1.00** | **1.37** | **2.18** | **1.70** | **0.60** |

## Appendix D: Risk Register

| Work Package | WP no. | Ref no. | Risk Description | Potential impact on project | Risk Probability (%) | Inherent Risk Score L | Inherent Risk Score I | Inherent Risk Score Total (LxI) | Level | Mitigation | Schedule impact mths | Mitigation costs £k | Risk probability x mitigation costs (£k) |
|---|---|---|---|---|---|---|---|---|---|---|---|---|---|
| Software | WP1 | 1 | GRID tools and infrastructure not reliable for large scale simulations | Inability to perform external background simulations | 10% | 2 | 2 | 4 | Medium | Use alternative batch farms (e.g. TACC in Texas). | 0 | 0 | 0 |
| Software | WP1 | 2 | Muon and neutron induced background simulations not provided in timely manner | Passive and active shielding not optimized | 15% | 2 | 2 | 4 | Medium | Collaboration with Zaragoza, Sheffield and other ILIAS groups. | 0 | 0 | 0 |
| Tracker cell production/ Tracker frame | WP2 & 3 | 3 | Delays in sourcing materials due to delays in radiopurity approval | Manufacture of Tracker Module delayed | 20% | 2 | 3 | 6 | Medium | Work closely with Bordeaux experts and tests materials a.s.a.p. | 6 | 160 | 32 |
| Tracker cell production | WP2 | 4 | Delays in/unsatisfactory wire preparation | Cell production delayed | 5% | 1 | 3 | 3 | Low | Test wired cells in small batches | 3 | 80 | 4 |
| Tracker cell production | WP2 | 5 | Full automation of wiring delayed/failed | Longer construction period, higher cost, risk of radioactive contamination | 15% | 2 | 4 | 8 | Medium-High | Distributed production of tracking cells, stricter radiopurity control | 12 | 400 | 60 |
| Tracker cell production | WP2 | 6 | Tracker testing technology too slow. | Construction delayed. | 30% | 3 | 2 | 6 | Medium | Redundancy in testing technology (cosmics + source + laser) | 8 | 220 | 66 |
| Tracker cell production | WP2 | 7 | Cell failure during transportation | Rework required to replace damaged cells | 10% | 2 | 3 | 6 | Medium | Careful design of transport container | 3 | 40 | 4 |
| Tracker frame | WP3 | 8 | Manufacturing delays for Tracker frame | Construction delayed. | 10% | 2 | 3 | 6 | Medium | Close monitoring of sub-contractors | 6 | 160 | 16 |
| Tracker cell production/ Tracker frame | WP2 & 3 | 9 | Cell contamination during production and assembly process | Rework required to clean/replace contaminated cells | 15% | 2 | 3 | 6 | Medium | Ensure cleanroom facilities and procedures are strictly controlled. | 3 | 40 | 6 |
| Tracker frame | WP3 | 10 | Failure of Tracker Module | Project delayed | 10% | 2 | 4 | 8 | Medium-High | Test smaller sections of the Tracker Module during assembly phase | 12 | 400 | 40 |

| Work Package | WP no. | Ref no. | Risk Description | Potential impact on project | Risk Probability (%) | Inherent Risk Score L | I | Total (LxI) | Level | Mitigation | Schedule impact mths | Mitigation costs £k | Risk probability x mitigation costs (£k) |
|---|---|---|---|---|---|---|---|---|---|---|---|---|---|
| Tracker Readout | WP4 | 11 | Delay in specifying constraints | Design delayed | 10% | 2 | 2 | 4 | Medium | Reorganise project to bring forward well specified areas and delay less well specified areas | 2 | 20 | 2 |
| Tracker Readout | WP4 | 12 | Failure of prototypes | Production delayed, increased costs | 5% | 1 | 2 | 2 | Low | Respin | 1 | 20 | 1 |
| Tracker Readout | WP4 | 13 | Delays in ASIC design | Readout delayed | 10% | 2 | 3 | 6 | Medium | Alternate contractor | 2 | 15 | 2 |
| Tracker Readout | WP4 | 14 | Delays in ASIC production | Readout delayed, additional costs | 5% | 1 | 3 | 3 | Low | Alternate foundry | 2 | 15 | 1 |
| Tracker Readout | WP4 | 15 | Delays in commissioning | Readout delayed | 10% | 2 | 2 | 4 | Medium | Add manpower | 2 | 15 | 2 |
| General | N/A | 16 | Natural disaster or accident (e.g. fire) | End of Project | N/A | 1 | 5 | 5 | Medium | Design equipment with strict safety specifications. | 0 | 0 | 0 |
| General | N/A | 17 | Damage of major component during transportation, installation. | Delay to schedule. | 10% | 2 | 2 | 4 | Medium | Packing, handling and contingency. | 3 | 40 | 4 |
| General | N/A | 18 | Loss of key staff | Delay to schedule. | 10% | 2 | 3 | 6 | Medium | Shared responsibilities. | 3 | 40 | 4 |
| General | N/A | 19 | Loss of supplier. | Delay to schedule. | 5% | 1 | 3 | 3 | Low | Identify alternative suppliers. | 3 | 40 | 2 |
| General | N/A | 20 | Major price fluctuations. | Higher cost. | N/A | 1 | 3 | 3 | Low | Plan for descoping | N/A | N/A | 0 |
| | | | | | | | | | | | | Total | 245 |

L = Likelihood on scale of 1, 2 ,3 4 where 1 is low.
I = Impact on scale of 1, 2, 3, 5 where 1 is low.

High risk is a total score greater than 8

Contingency: 10% of total budget

# Bibliography

1. H.V. Klapdor-Kleingrothaus and I.V. Krivosheina, Modern Physics Letters A, Vol. 21, No. 20 (2006) 1547{1566

2. See for example “Massive Neutrinos in Physics & Astrophysics” (World Scientific Lecture Notes in Physics: Vol. 72), R.N. Mohapatra and P.B. Pal (World Scientific Publishing, 2002).

3. See for example the PDG review of neutrino mixing : http://pdg.lbl.gov/2008/reviews/rpp2008-rev-neutrino-mixing.pdf

4. F.Feruglio, A.Strumia and F.Vissani, “Neutrino oscillations and signals in β and 0νββ experiments,” Nucl. Phys. B **637** (2002) 345.

5. J.Schechter and J.W.F.Valle, “Neutrinoless double-beta decay in SU(2) x U(1) theories,” Phys. Rev. D **25**, 2951 (1982).

6. http://nemo.in2p3.fr/publications/

7. A.S.Barabash, “Double-beta-decay experiments: Present status and prospects for the future,” Phys. Atom. Nucl. **67** (2004) 438.

8. R. Arnold et al., “Probing New Physics with SuperNEMO, submitted to EPJ, April 2010.

9. E. Chauveau [SuperNEMO Collaboration], AIP Conf. Proc. 1180, 26 (2009).

10. A. Nachab, “Radon reduction facility and Radon measurements at the ModaneUnderground Laboratory”, 2nd Topical Workshop on Low Radioactivity, October, 2006, Aussois, France.